EDGEWOOD

RESEARCH, DEVELOPMENT & ENGINEERING CENTER

U.S. ARMY CHEMICAL AND BIOLOGICAL DEFENSE COMMAND

ERDEC-CR-199
(GC-TR-94-2250)

CATALYTIC OXIDATION OF HYDROGEN CYANIDE OVER A MONOLITHIC OXIDATION CATALYST

J.A. Rossin

GEO-CENTERS, INC.
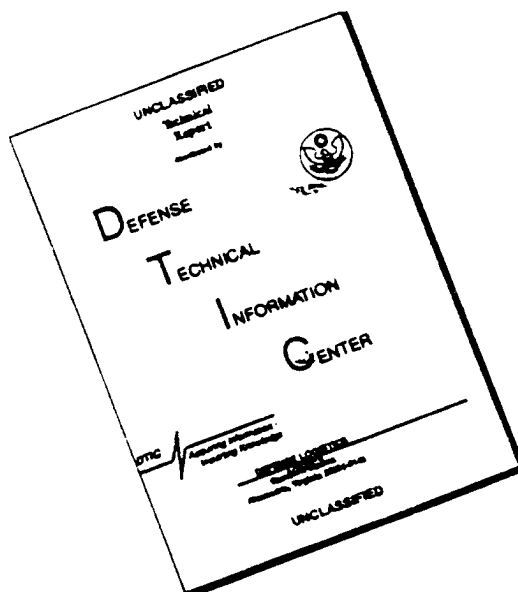Ft. Washington, MD 20744

October 1995

19960404 034

Aberdeen Proving Ground, MD 21010-5423

DTIC QUALITY INSPECTED 1

DISCLAIMER NOTICE

THIS DOCUMENT IS BEST QUALITY AVAILABLE. THE COPY FURNISHED TO DTIC CONTAINED A SIGNIFICANT NUMBER OF PAGES WHICH DO NOT REPRODUCE LEGIBLY.

Disclaimer

The findings in this report are not to be construed as an official Department of the Army position unless so designated by other authorizing documents.

REPORT DOCUMENTATION PAGE

1. AGENCY USE ONLY (Leave blank)	2. REPORT DATE 1995 October	3. REPORT TYPE AND DATES COVERED Final, 93 Nov - 94 Mar

4. TITLE AND SUBTITLE

Catalytic Oxidation of Hydrogen Cyanide Over a Monolithic Oxidation Catalyst

5. FUNDING NUMBERS

C-DAAA15-91-C-0075

6. AUTHOR(S)

Rossin, J.A.

7. PERFORMING ORGANIZATION NAME(S) AND ADDRESS(ES)

Geo-Centers, Inc., Ft. Washington, MD 20744

8. PERFORMING ORGANIZATION REPORT NUMBER

ERDEC-CR-199
(GC-TR-94-2250)

9. SPONSORING · MONITORING AGENCY NAME(S) AND ADDRESS(ES)

DIR, ERDEC, ATTN: SCBRD-RTE, APG, MD 21010-5423

10. SPONSORING / MONITORING AGENCY REPORT NUMBER

11. SUPPLEMENTARY NOTES

COR: Dr. David Tevault, SCBRD-RTE, (410) 671-8400

12a. DISTRIBUTION / AVAILABILITY STATEMENT

Approved for public release; distribution is unlimited.

12b. DISTRIBUTION CODE

13. ABSTRACT (Maximum 200 words)

The catalytic oxidation of hydrogen cyanide was evaluated over a monolithic oxidation catalyst at temperatures between 220 and 310°C in air employing feed concentrations between 200 and 20,000 ppm (241 and 24,100 mg/m^3). Isothermal reaction rate data were measured by exposing the catalyst to various concentrations of hydrogen cyanide and recording the conversion as a function of residence time. Reaction rate data were correlated using a mathematical model, which took into account external mass transfer resistances and kinetic effects. Data were also recorded under conditions representative of a chemical attack, which were simulated in the laboratory by exposing the catalyst to high concentration pulse challenges of hydrogen cyanide. Catalytic deactivation resulting from the oxidation of hydrogen was insignificant. Reaction products consisted of CO_2, N_2, N_2O, and NO_x, with the formation of NO_x being favored at high reaction temperatures. The rate of hydrogen cyanide oxidation was highly non-linear in the concentration of hydrogen cyanide, with the reaction rate being inversely proportional to the concentration of hydrogen cyanide at high concentrations. Results of the pulse testing demonstrated that hydrogen cyanide is highly reactive, and that high concentrations of hydrogen cyanide may be completely oxidized at reaction temperatures between 350-375°C.

14. SUBJECT TERMS

Air purification	Catalyst
Catalytic oxidation	Catox
Fixed-bed reactor	

15. NUMBER OF PAGES

53

16. PRICE CODE

17. SECURITY CLASSIFICATION OF REPORT UNCLASSIFIED	18. SECURITY CLASSIFICATION OF THIS PAGE UNCLASSIFIED	19. SECURITY CLASSIFICATION OF ABSTRACT UNCLASSIFIED	20. LIMITATION OF ABSTRACT UL

Blank

PREFACE

The use of trade or manufacturers' names in this report does not constitute an official endorsement of any commercial products. This report may not be cited for purposes of advertisement.

This report has been approved for public release. Registered users should request additional copies from the Defense Technical Information Center; unregistered users should direct such requests to the National Technical Information Service.

Acknowledgments

3

Blank

CONTENTS

FIGURES

7

CATALYTIC OXIDATION OF HYDROGEN CYANIDE OVER A MONOLITHIC OXIDATION CATALYST

1. INTRODUCTION

Present air purification systems designed for removal of chemical warfare agents from air streams are based solely on activated, impregnated carbon, namely ASC whetlerite. While these filters function well against a wide range of chemical agents, they possess several shortcomings. First, the carbon filter has a limited capacity for agents which are removed by chemical reaction and those which are weakly adsorbed. Second, prolonged environmental exposure has been shown to reduce the capacity of these filters for agents which are removed by chemical reaction as a result of chromium(VI) reduction[1]. The result of these shortcomings is to impose change-out and potential disposal requirements which may present logistical as well as disposal burdens to the user. Catalytic oxidation is an alternative air purification technology which is being investigated as a means of alleviating the above mentioned burdens.

The nature of a chemical attack coupled with the high toxicity of agent molecules makes the separation of chemical agents from streams of air a complex process. During a chemical attack, high concentrations (in excess of 1%) of nonpersistent gases may be achieved within a few seconds, and can be maintained for a few minutes prior to decay[2]. When confronted with a rapid change in concentration, a catalytic air purification unit would be expected to behave as follows. Initially, the catalyst bed is at a temperature consistent with that of the inlet air. At the onset of the chemical attack, the temperature of the catalyst bed will rapidly increase, due to the heat of combustion of the challenge vapor. The rapid increase in the catalyst temperature will result in an equally rapid increase in catalyst's performance; i.e., the effluent concentration of agent will decrease over the duration of the chemical attack. The lethality of a compound is determined by its toxicity and the dose received, i.e., the product of concentration and exposure time (ct), usually expressed in $mg\text{-}min/m^3$. For hydrogen cyanide, the Lct(50) and "no effect" doses are reported to be 2,000 and 11 $mg\text{-}min/m^3$, respectively. Lct(50) is defined as the dose of chemical agent which will be lethal to 50% of the subjects exposed.

The objective of this study was to develop an experimentally based reactor design equation which would be capable of estimating the size and energy requirement of a full scale catalytic air purification unit. The approach taken in meeting this objective was to first record isothermal reactor design data over a wide range of temperatures, concentrations and residence times, and then correlate the design data using a mathematical model which takes into account all necessary transport resistances and kinetic effects. Following this, the performance of the catalyst would be evaluated under realistic chemical attack scenarios, and the data obtained from these tests would be compared to that predicted by a mathematical model. Also included in this effort was quantitatively identifying all reaction products formed during the oxidation of hydrogen cyanide.

2. EXPERIMENTAL METHODS

Materials: Hydrogen cyanide was purchased from Matheson Gas in 1A compressed gas cylinders diluted with helium such that the concentration of hydrogen cyanide was approximately 7.5% (v/v). Analysis revealed the compound to be greater than 99% pure. The gas was purchased in helium, rather than air, so that the concentration of N_2, a potential reaction product, could be assessed. Calibration gases (namely CO and CO_2 in air) were also obtained from Matheson.

Catalyst Preparation: Catalyst cores were cut from a 30 cm diameter by 10.2 cm long monolith block using a diamond tip hole saw. For the isothermal reaction rate studies, a 1.95 cm diameter by 5.0 cm long catalyst core was employed, while the transient studies employed a 3.5 cm diameter by 10.4 cm long catalyst core. For the isothermal monolith studies, the center channels of the monolith were plugged with alundum cement so that only the channels near the outer circumference of the catalyst core (totaling 86 channels) remained open. For the isothermal reaction rate studies, the catalyst volume was 4.62 cm^3. For the transient studies, all channels of the monolith remained unobstructed, with the catalyst volume being 103.2 cm^3. Both catalyst cores were wrapped with a thin layer of glass wool and loaded into the reactor. The glass wool was used to maintain a seal between the catalyst and the reactor wall to prevent catalyst by-pass. Once loaded into the reactor, type K fine wire thermocouples were extended axially into the channels of the monolith at discrete locations. For the catalyst core employed in the isothermal rate studies, 6 thermocouples were placed within channels of the monolith and located 1.0 cm upstream of the catalyst, and within the catalyst at 0.5, 1.0, 2.0, 3.0 and 4.0 cm from the inlet. All thermocouples located within the catalyst occupied channels near the outer circumference. For the catalyst core employed in the transient studies, a total of 10 thermocouples extended into the channels of the monolith. These thermocouples were located 1 cm upstream and downstream of the monolith, and 0.5, 1.5, 2.5, 4.0, 6.0, 8.0 and 10.0 cm from the inlet. All thermocouples occupied channels near the center of the monolith. In addition, two thermocouples were located at 1.5 and 4.5 cm from the inlet of the monolith near the outer diameter. These thermocouples were used to assess radial temperature gradients.

Equipment: A schematic representation of the fixed bed reactor system is illustrated in Figure 1. Dry, oil-free air from a PSA air drier was metered to the reactor using either a 0-5 or 0-20 Nl/min mass flow controller. Nl is defined as one liter of dry air at 0°C and one atmosphere pressure. Dry air from the mass flow controller was then delivered to a water saturator, which was housed in a temperature controlled chamber. A back pressure regulator is located downstream of the water saturator. The concentration of water in the air stream may be controlled by controlling the temperature and pressure of the water saturator. In addition, the water saturator could be by-passed to conduct the experiments in dry air.
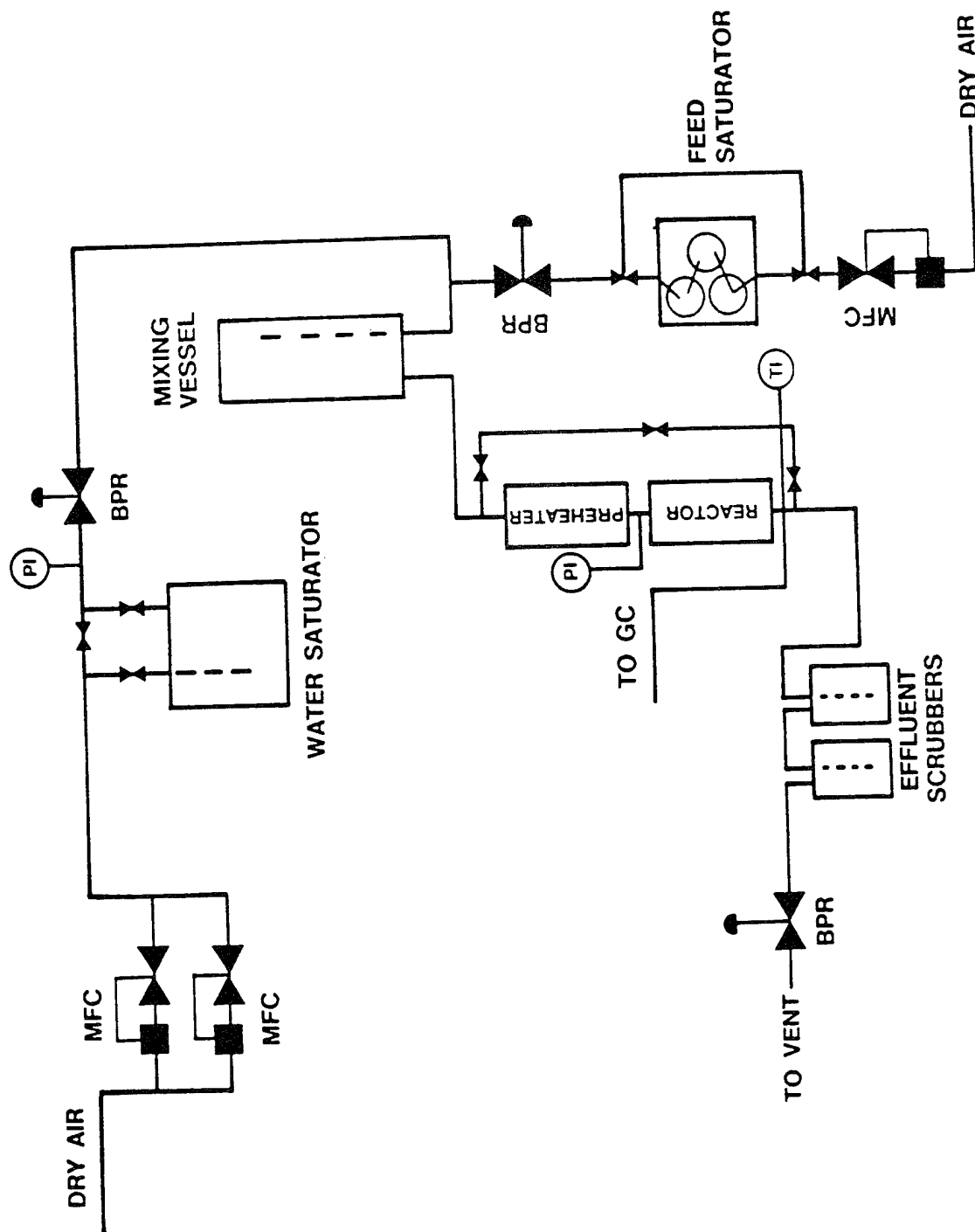
10

Figure 1: Schematic Representation of Fixed Bed Catalytic Reactor System. BPR: back pressure regulator; GC: gas chromatograph; MFC: mass flow controller.

Hydrogen cyanide was delivered to the air stream from a compressed gas cylinder containing approximately 7.5% hydrogen cyanide in helium. The reactant stream was metered into the humidified air stream via one of three mass flow controllers; 0-50 Nml/min, 0-200 Nml/min and 0-2,000 Nml/min. In some cases, the 0-2,000 Nml/min flow controller was replace with a 0-5,000 Nml/min controller. Use of this flow controller bank allowed for achieving a wide range of concentrations over the desired air flow rate range.

Once blended, the feed stream was delivered to the catalytic reactor. The reactor consisted of a 66 cm long glass tube (2.54 cm o.d. for the reaction rate studies, 3.8 cm o.d for the transient studies). The upper 40 cm of the glass reactor served as the pre-heat zone and was filled with 4 mm diameter glass beads. The glass beads provide further mixing of the feed gas as well as surface area for improving the heat transfer properties of the unit. The reactor tube was housed in an 8.9 cm diameter by 60 cm long aluminum block. The aluminum block was electrically heated, and the temperature of the reactor was controlled by controlling the temperature of the aluminum block. The catalyst core was located approximately 7 to 10 cm below the pre-heat zone of the reactor.

Following the reactor, the effluent stream was delivered to two scrubber tanks in series. The scrubber tanks were filled approximately half way with 10 molar sodium hydroxide solution and served to remove acid gases from the effluent stream. Flow from the scrubber vessels was delivered to a back pressure regulator, which served to maintain a constant pressure on the reactor. Flow from the back pressure regulator was vented within a fume hood. All lines in contact with hydrogen cyanide were contained within the fume hood and were electrically heat traced.

During the transient studies, the reactor system was modified to deliver a pulse challenge of hydrogen cyanide to the catalyst bed. Modifications to the system included installing a three-way valve between the mass flow controllers (used to deliver hydrogen cyanide) and the junction with the air stream. The three-way valve allows one to divert reactant flow to the air stream prior to the reactor, or by-pass the reactor and divert the reactant flow to vent.

Isothermal Reaction Rate Measurements: Reaction rate data were recorded at temperatures of 200, 230, 260, 290 and 310°C at a pressure of 6±1 psig. The feed concentration of hydrogen cyanide was varied between 200 and 20,000 ppm (241 and 24,100 mg/m^3) in dry air. Dry air was used because screening studies indicated that the addition of water to the air stream (T_{dew} = 21±1°C) did not influence the catalytic reactivity. In addition, selected experiments were performed at 290°C at pressures of 6, 15 and 23 psig employing a feed concentration of 5,000 ppm (6,025 mg/m^3) in air. The residence time, based on the reactor volume occupied by the unobstructed monolith channels and calculated at 0°C and 1 atm pressure, was adjusted in an effort to achieve conversions between 20 and 90%. Air flow rates were typically varied between 2 and 25 Nl/min. In addition, oxygen was added to the feed stream whenever hydrogen cyanide concentrations greater than 5,000 ppm were employed. This was necessary, since the

hydrogen cyanide was diluted in helium, and it was desired that the experiments be conducted in 21% oxygen. Reaction rate data were recorded only during day-time hours. Overnight, the catalyst was maintained at reaction temperature under flowing air. The same catalyst core was used for all experiments conducted in this study. All process conditions were maintained for between 1 to 3 hours to ensure the achievement of steady-state. It should be noted that for feed concentrations greater than 1,000 ppm, an increase in the catalyst temperature was observed. In these instances, the catalyst temperature was adjusted such that the average catalyst temperature (numerical average based on the thermocouple measurements) was $\pm 2°C$ of the desired value. Both feed and effluent were analyzed continuously for CO_2 and reactant during all runs. The conversion of hydrogen cyanide was determined based on the concentration of hydrogen cyanide in the feed and effluent streams.

Transient Rate Measurements: The procedure used to record transient rate data has been reported elsewhere for the oxidation of chloroacetonitrile[4]. Transient rate data were recorded at air inlet temperatures of 290, 310, 330, and 350°C in a humid helium/ oxygen mixture at a pressure of 6 ± 1 psig at residence times between 0.25 and 0.5 second. Helium was chosen rather than nitrogen because helium is more compatible with the mass selective detector associated with the mass spectrometer (MS) used to analyze the concentration of hydrogen cyanide in the effluent. Feed concentrations between 5,000 and 27,500 ppm (6,025 and 33,100 mg/m^3) were evaluated. Runs were performed by exposing the catalyst to pulse challenges of hydrogen cyanide while recording feed and effluent concentrations, and catalyst temperature at several thermocouple locations during the challenge in real-time. A pulse challenge of hydrogen cyanide was delivered to the system as follows. First, with humid He/O$_2$ flowing through the reactor at the desired flow rate and temperature, reactant flow was initiated and vented for approximately five minutes prior to the pulse introduction. The run was initiated by diverting the reactant flow (using the three-way valve) to the He/O$_2$ stream at a junction prior to the reactor. The run was terminated following the three minutes of challenge by returning the reactant stream to its initial position (flow by-passing the catalyst). At this time, the reactant flow was discontinued. During the challenge, the concentration of hydrogen cyanide in the feed and effluent streams and the catalyst temperature were recorded simultaneously in real-time.

Runs were also conducted to evaluate the reaction products over the course of the challenge. During the pulse challenge, a portion of the reactor effluent was diverted to a NO/NO$_x$ analyzer (chemilumenescence detector), which was modified to record either the NO or NO$_x$ concentration in real-time. In order to obtain the concentration of each compound, the run was repeated, first with the analyzer in the NO mode, then with the analyzer in the NO$_x$ mode. It should be noted that the MSD could not be used to record the concentrations of reaction products, due to fragment interference with parent ions. For example, N$_2$O fragments consisted of N$_2$ and NO, and NO$_2$ fragments consisted of NO.

Sample Analysis: During the reaction rate studies, the concentration of hydrogen cyanide in the feed and effluent stream, and the concentration of CO_2 in the effluent stream were monitored. All analyses were performed using a Hewlett-Packard 5890 gas chromatograph (GC) equipped with both a flame ionization detector (FID) and a thermal conductivity detector (TCD) and automatic sampling valves. Hydrogen cyanide was analyzed using a 2 m by 3.2 mm diameter Krytox GC column attached to the FID, while CO_2 was analyzed using a 2 m by 3.2 mm diameter Heysep Q column attached to the TCD. Samples were analyzed first by sampling the effluent for CO_2 at 50°C, then heating the oven to 125°C at 32.5°C/min and sampling the effluent for hydrogen cyanide. Following this, the feed stream is sampled for hydrogen cyanide. The above analysis sequence required 16 minutes to perform. A sample of the GC trace is reported in Figure 2. It should be noted that later testing discovered that a Heysep Q column operated at 100 to 120°C provides an improved analyses of hydrogen cyanide.

During the transient rate studies, the concentration-time profile of hydrogen cyanide in the feed stream was determined using the FID detector of the GC. A 50 Nml/min portion of the feed stream was diverted through a mass flow controller and delivered directly to the FID without passing through a GC column. The concentration vs. time profile of the feed was obtained from the FID signal recorded on a Hewlett-Packard 3396A integrator. Catalyst temperatures from each thermocouple were monitored in real-time using an Omega OM500 multi-channel data logger. This unit reported all temperatures simultaneously at 5 second intervals. Immediately following the reactor, a portion of the effluent stream was delivered to a Hewlett-Packard 5971A mass spectrometer (with a mass selective detector) for analysis. Effluent concentrations of hydrogen cyanide were quantitatively determined by continuously monitoring the parent ion (MW = 27) of hydrogen cyanide. Both the FID and mass selective detector were calibrated daily.

3. MODEL DEVELOPMENT AND FIT PARAMETER ESTIMATION

Reaction Rate Model Development: The monolithic oxidation catalyst employed in this study consisted of a series of straight, parallel channels. The monolith substrate is coated with a thin layer of catalyst support material, termed washcoat. The catalyst particles are impregnated onto the washcoat. The monolith employed in this study had square channels, with a channel density 93 cells/cm². The thickness of the washcoat and substrate were not supplied by the manufacturer. For modeling purposes, the washcoat was assumed to be 0.0035 cm thick, and the substrate was assumed to be 0.0115 cm thick. A schematic representation of a monolith channel is provided below in Figure 3. Based on these dimensions, the monolith is 11.55% washcoat plus catalyst.

RUN # 5A2   NOV 23, 1993   11:12:37
START

N2 3.795
P1 3.83 H2O
3.258 CO2   HCN effluent   9.858
                HCN feed
                                 13.895
STOP

Run 11-23c-93
LCJ = 1,650 ppm
Υ = .014 seconds
T ≈ 287°C

1.055

Closing signal file M:SIGNAL.BNC

RUN# 5A2   NOV 23, 1993   11:12:37

SIGNAL FILE: M:SIGNAL.BNC
AREA%

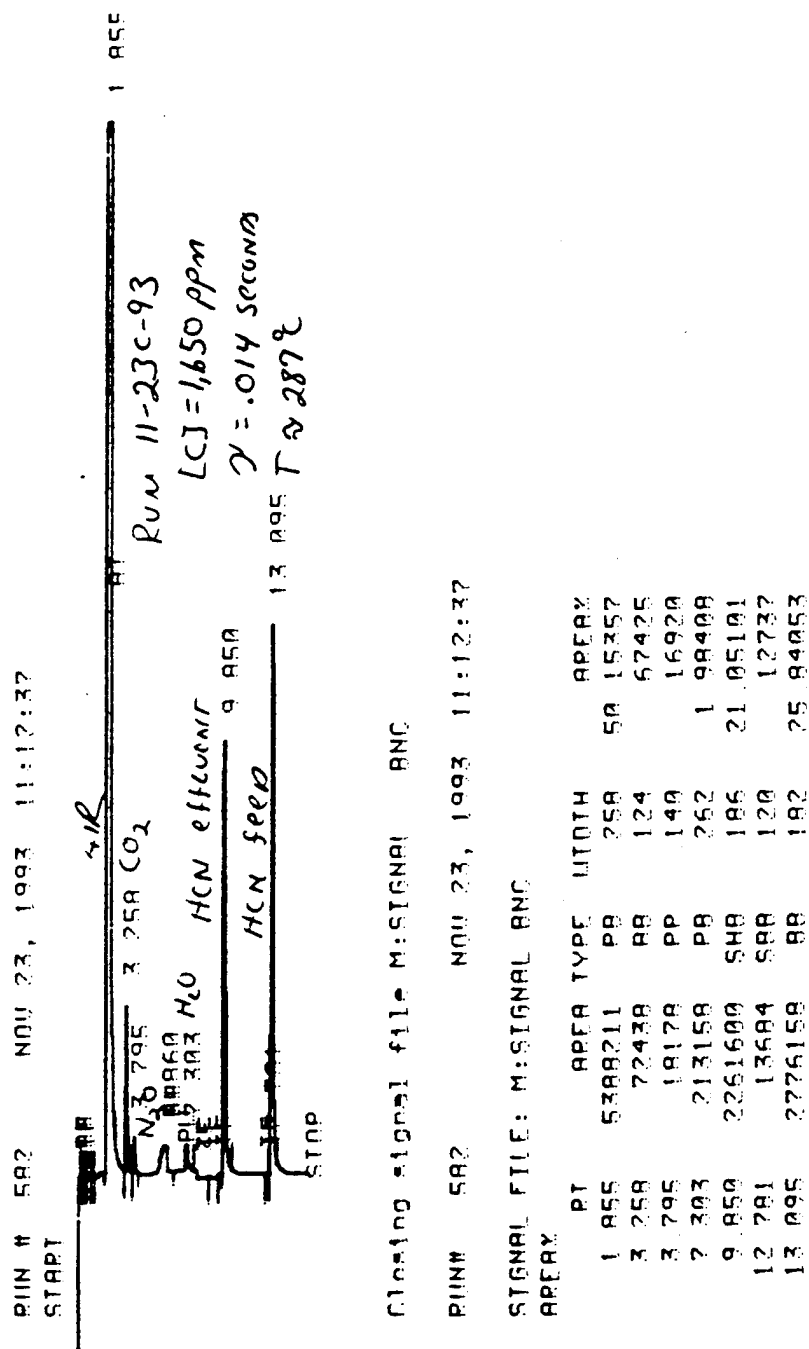| RT	AREA	TYPE	WIDTH	AREA%
1.055	5388211	PB	.258	50.15357
3.258	72438	BB	.124	.67425
3.795	18178	PP	.140	.16920
7.383	2131598	PB	.252	1.99408
9.858	2261688	SHB	.186	21.05101
12.781	13684	SBB	.128	.12737
13.895	2776158	BB	.192	25.84853

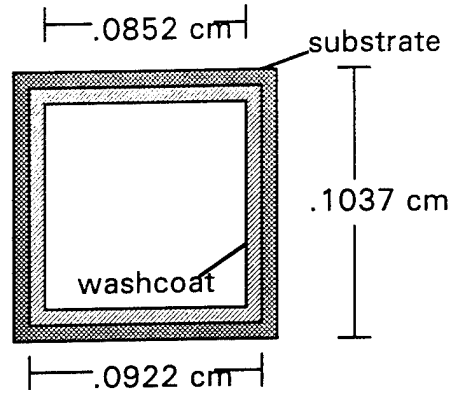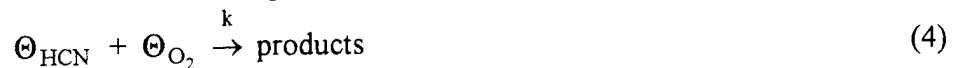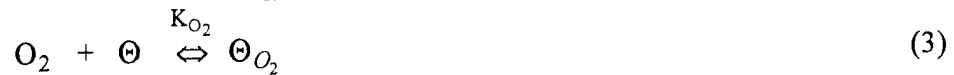Figure 2: GC Trace of Feed and Effluent Analysis.

Figure 3: Schematic Representation of a Monolith Channel.

The oxidation of hydrogen cyanide was modeled according to the reaction rate expression:

$$\text{Rate} = \frac{AC_{HCN}}{(1 + BC_{HCN})^2} \tag{1}$$

In the above reaction rate expression, A and B are fit parameters (s^{-1} and cm^3/mol, respectively), C_{HCN} is the concentration of hydrogen cyanide ($mols/cm^3$) and rate is the reaction rate ($mols/s$-cm^3 catalyst). The reaction rate expression may be derived by assuming the reaction occurs between adsorbed hydrogen cyanide and adsorbed oxygen (Langmuir-Hinshelwood mechanism):

$$HCN + \Theta \overset{K_{HCN}}{\Leftrightarrow} \Theta_{HCN} \tag{2}$$

$$O_2 + \Theta \overset{K_{O_2}}{\Leftrightarrow} \Theta_{O_2} \tag{3}$$

$$\Theta_{HCN} + \Theta_{O_2} \overset{k}{\rightarrow} \text{products} \tag{4}$$

where Θ represents the fraction of vacant adsorption sites, and Θ_{HCN} and Θ_{O_2} represent the fraction of adsorption sites covered with adsorbed hydrogen cyanide and oxygen, respectively. K_{HCN}, K_{O_2} and k are the adsorption equilibrium constants for hydrogen cyanide and oxygen (cm^3/mol), and the reaction rate constant(s^{-1}), respectively. For the reaction to occur, an adsorbed hydrogen cyanide molecule must be adjacent to an adsorbed oxygen molecule. According to equations 2 through 4, the reaction rate expression becomes:

$$\text{Rate} = k\Theta_{HCN}\Theta_{O_2} \tag{5}$$

Since the concentrations of hydrogen cyanide and oxygen adsorbed onto the surface of the catalyst are unknown, we must solve for these concentrations in terms of the gas phase

concentration using adsorption equilibrium constants. At equilibrium, the rate of adsorption equals the rate of desorption, so that:

$$\Theta_{O_2} = K_{O_2} C_{O_2} (1 - \Sigma\Theta) \tag{6}$$

$$\Theta_{HCN} = K_{HCN} C_{HCN} (1 - \Sigma\Theta) \tag{7}$$

Equations 6 and 7 state that the fraction of sites covered with either hydrogen cyanide or oxygen is equal to the adsorption equilibrium constant times the respective gas phase concentration times the fraction of vacant sites $(1 - \Sigma\Theta)$. $\Sigma\Theta$ represents the fraction of sites covered with adsorbed hydrogen cyanide and oxygen. In order to solve for the fraction of sites covered with either adsorbed hydrogen cyanide or oxygen, the term $(1 - \Sigma\Theta)$ must first be solved for. This is accomplished by first adding equations 6 and 7:

$$\Sigma\Theta = (K_{HCN} C_{HCN} + K_{O_2} C_{O_2})(1 - \Sigma\Theta) \tag{8}$$

followed by subtracting both sides from unity:

$$1 - \Sigma\Theta = 1 - (K_{HCN} C_{HCN} + K_{O_2} C_{O_2})(1 - \Sigma\Theta) \tag{9}$$

Dividing both sides of the equation by $(1 - \Sigma\Theta)$ and re-arranging yields the solution for $(1 - \Sigma\Theta)$:

$$1 - \Sigma\Theta = \frac{1}{1 + K_{O_2} C_{O_2} + K_{HCN} C_{HCN}} \tag{10}$$

Substituting eq. 10 into eqs. 6 and 7 yields the fractional site coverage of hydrogen cyanide and oxygen, Θ_{HCN} and Θ_{O_2}, respectively, in terms of their gas phase concentrations. Substituting this result into eq. 5 yields a reaction rate expression which describes a reaction between adsorbed hydrogen cyanide and adsorbed oxygen:

$$Rate = \frac{kK_{O_2} K_{HCN} C_{O_2} C_{HCN}}{(1 + K_{O_2} C_{O_2} + K_{HCN} C_{HCN})^2} \tag{11}$$

The concentration of oxygen was held constant during all experiments (21%) and was in great excess (meaning that regardless of the hydrogen cyanide conversion, the concentration of oxygen did not change significantly over the length of the reactor). Therefore, the term $1 + K_{O_2} C_{O_2}$ can be treated as a constant and divided from the above rate expression (eq. 11):

$$Rate = \frac{AC_{HCN}}{(1 + BC_{HCN})^2} \tag{12}$$

17

where the constants A and B are:

$$A = \frac{kK_{O_2}K_{HCN}C_{O_2}}{(1 + K_{O_2}C_{O_2})^2} \tag{13}$$

$$B = \frac{K_{HCN}}{1 + K_{O_2}C_{O_2}} \tag{14}$$

Gland et al.[5] have shown that oxygen is strongly adsorbed onto the surface of platinum at temperatures between -123 and 427°C. Therefore, the oxygen adsorption term $(K_{O_2}C_{O_2})$ is much greater than unity, and the constants A and B reduce to.

$$A = \frac{kK_{HCN}}{K_{O_2}C_{O_2}} \tag{15}$$

$$B = \frac{K_{HCN}}{K_{O_2}C_{O_2}} \tag{16}$$

Note that the fit parameters A and B are inversely proportional to the oxygen concentration (and therefore the total pressure). Therefore, in extrapolating the rate expression to conditions of greater total pressure and/or oxygen concentration, the fit parameters must be adjusted accordingly, since both A and B are inversely proportional to the oxygen concentration.

The above rate expression was incorporated into a fixed bed reactor design equation which took into account external mass transfer resistances and kinetic effects. The equations which govern mass transfer and chemical reaction rates within the channel of the monolith are[6]:

$$\bar{v}\frac{dC_{HCN}^g}{dz} = k_mA[C_{HCN}^s - C_{HCN}^g] \tag{17}$$

$$Rate = k_mA'[C_{HCN}^g - C_{HCN}^s] \tag{18}$$

where $\bar{v}$ is the average linear velocity within the channel at reaction conditions (cm/s), C_{HCN}^g and C_{HCN}^s refer to the gas and solid phase concentration of hydrogen cyanide, respectively, calculated at reaction conditions (mols/cm^3), z is the differential reactor length (cm), k_m is the mass transfer coefficient (cm/s), A is the surface area of the monolith channel (cm^2/cm^3 void), Rate is the reaction rate as defined in eq. 1 (mols/s-cm^3-cat), and A' is the surface area of the catalyst (cm^2/cm^3 catalyst). The above reaction rate expressions were integrated numerically using a multistep method. Fit parameters were determined by minimizing the error between the residence time and the residence

18

time required to achieve the experimental conversion. This method was selected versus minimizing the error between the predicted and experimental conversion, since for conversions greater than about 40%, small changes in the residence time can have a significant effect on the conversion (see Results and Discussion section). Data were correlated over the entire data set simultaneously, rather than by the standard technique of determining the fit parameters at each reaction temperature, followed by correlating the data using Arrhenius type equations. The mass transfer coefficient was determined from a limiting Sherwood number correlation[7]:

$$Sh = 3.66(1 + 0.95 ReSc\frac{d}{z})^{0.45} \qquad (19)$$

$$k_m = \frac{ShD_{ab}}{2R_h} \qquad (20)$$

where Sh is the Sherwood number, Re is the Reynolds number, Sc is the Schmidt number, d is channel diameter (cm), D_{ab} is the diffusion coefficient for hydrogen cyanide in air (cm²/s), and R_h is the hydraulic radius of the channel (cm). The diffusion coefficient was 0.173 cm²/s at 0°C and was allowed to increase proportional to temperature to the power of 1.5 ($T^{1.5}$). Using the reactor design equations, the fit parameters were determined to be:

$$A = 1.7795(11) \exp(-18,433/RT)/P \text{ s}^{-1}$$
$$B = 3.0430(06) \exp(+ 4,435/RT)/P \text{ cm}^3/\text{mol}$$

Where P is the total pressure in atmospheres.

4. RESULTS AND DISCUSSION

Effects of Water: Figure 4 reports conversion as a function of temperature for the oxidation of 1,000 ppm (1,205 mg/m³) HCN in dry ($T_{dew} < -10°C$) and humid ($T_{dew} = 20°C$) air streams. (T_{dew} is the dew point temperature.) Data are reported for a residence time of 0.17 seconds at a total pressure of 6 psig. All residence times are reported relative to 0°C and one atmosphere pressure and are based on the volume of reactor occupied by the catalyst. Results show that water does not have an effect on the catalytic activity, to within experimental error. As a result, all experiments were conducted in dry air.

Reaction Products: The only carbon-containing reaction product identified in the reactor effluent stream was carbon dioxide. No carbon monoxide or products of partial oxidation were identified. Carbon balances averaged 98% for all runs conducted in this study. Figure 5 reports the product distribution of the nitrogen-containing reaction products as a function of temperature for the oxidation of 2,500 ppm hydrogen cyanide at atmospheric pressure. This test was conducted by placing a small piece of monolith into a 0.95 cm o.d. glass tube and performing the test in the micro-reactor system. In this
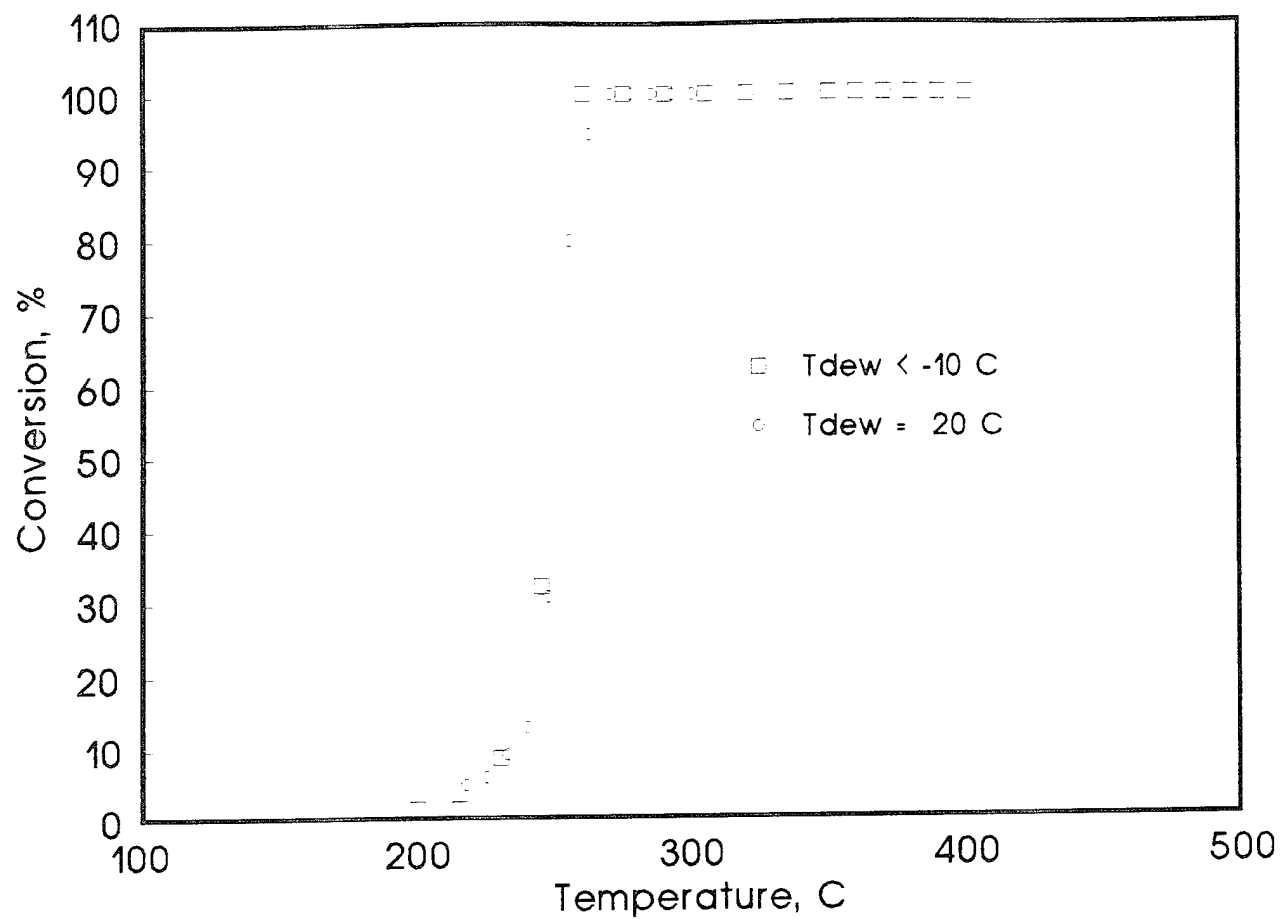
19

Figure 4: Conversion as a Function of Temperature for the Oxidation of Hydrogen Cyanide in Dry and Humid Air.
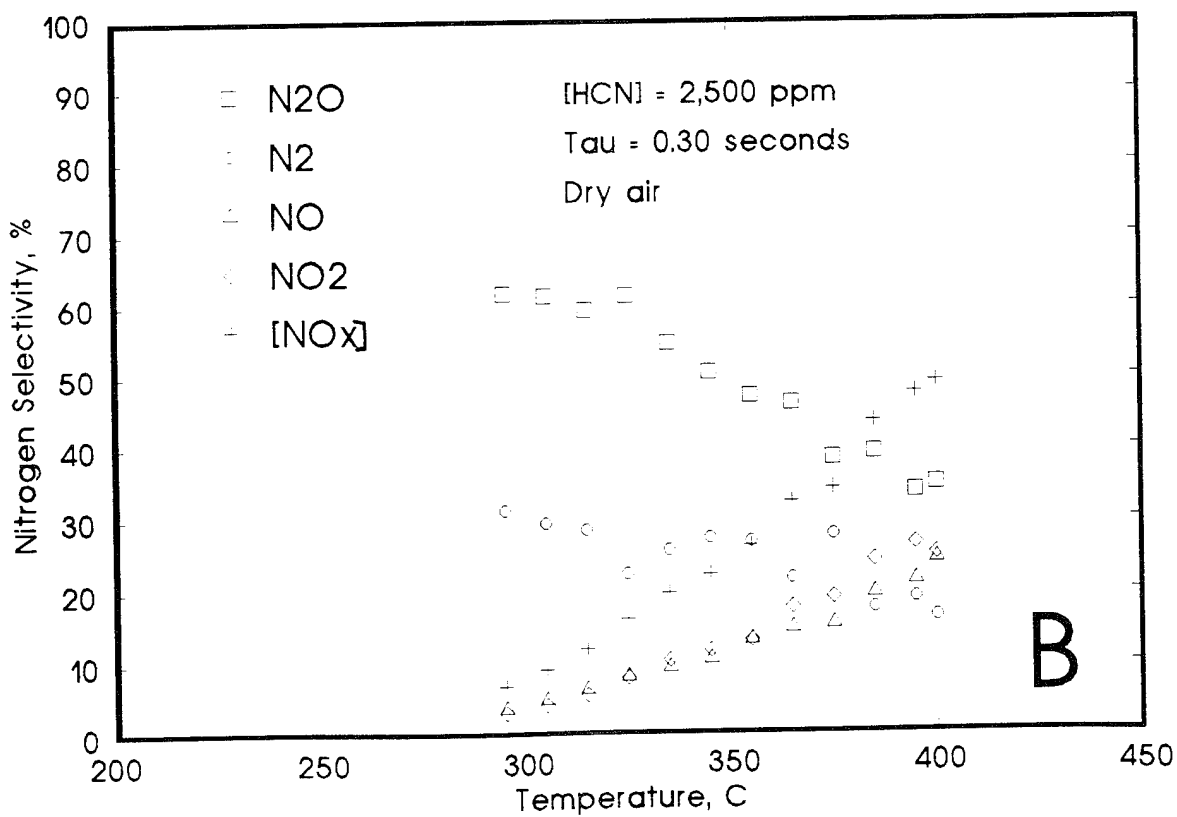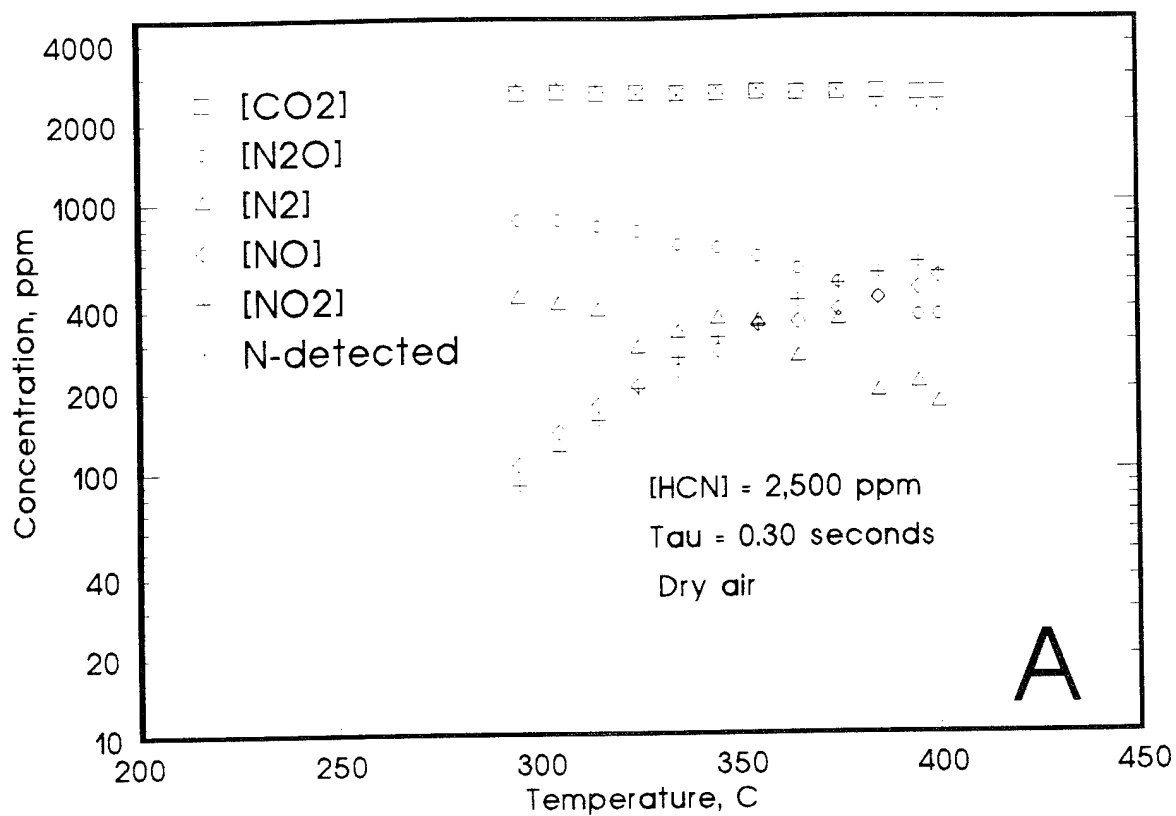
Figure 5: Concentration of Reaction Products (A) and Nitrogen Containing Reaction Product Distribution (B) as a Function of Temperature for the Oxidation of 2,500 ppm Hydrogen Cyanide in Dry Air.

21

manner, near isothermal operation could be achieved and the product distribution would not be skewed as a result of temperature effects. Nitrogen-containing reaction products consisted of N_2, N_2O, NO and NO_2, with NO plus NO_2 being collectively referred to as NO_x. The product distribution was found to vary as a function of temperature, with the formation of NO_x favored at high temperatures, and the formation of the reduced products (N_2 and N_2O) favored at the lower temperatures. Figure 5B reports the atomic nitrogen selectivity for hydrogen cyanide oxidation as a function of reaction temperature. At 400°C, approximately 50% of the nitrogen-containing products (on an atomic nitrogen basis) consist of NO_x. At temperatures below 300°C, NO_x selectivity below 10% was observed. The effects of hydrogen cyanide concentration and residence time were not evaluated during this testing effort. Residence time is not expected to have a significant effect on the product distribution, based on unpublished data involving the oxidation of acetonitrile.

Catalytic Deactivation: A continuous, long-duration deactivation test was not performed. Deactivation was assessed by returning to a set of initial conditions following over 100 hours of exposure to hydrogen cyanide, and comparing the results to those obtained earlier. Results indicated no loss of catalytic activity, to within experimental error. This result indicates that hydrogen cyanide will not deactivate the catalyst during multiple chemical attacks.

Reaction Rate Measurements: Oxidation reactions are highly exothermic. When recording reaction rate data, it is desired to minimize the heat transfer effects so that near isothermal operation is achieved. The result of this precaution is that the reaction rates are not masked by the heat transfer effects. For pelletted and granular catalysts, temperature excursions in the laboratory reactor can and often are controlled by diluting the catalyst bed with inert particles of a similar size. The monolithic catalyst, however, consists of a single piece of substrate and thus cannot be diluted in the same manner that granular catalysts are. Therefore, minimizing the axial temperature gradient presents a greater challenge to the investigator and may place limits on the experimental region which may be studied under near-isothermal conditions.

The oxidation of hydrogen cyanide in air is highly exothermic, with the heat of reaction (298 K) estimated to be 156 kcals/mol. From this value, the adiabatic temperature rises (for 100% conversion) corresponding to feed concentrations of 1,000, 3,000 and 10,000 ppm (1,205, 3,630 and 12,050 mg/m³) were calculated to be 20, 61 and 200°C, respectively. Because of the magnitude of the adiabatic temperature rise, difficulties in achieving near isothermal operation when operating with feed concentrations greater than 1,000 ppm were anticipated. In order to minimize the axial temperature gradients during the course of the testing, the center channels of the monolith were plugged with alundum cement so that only the channels at the outer circumference remained unobstructed.

Axial temperature gradients were assessed during each run from temperature measurements obtained using thermocouples located within channels near the center of the

monolith. Figure 6 reports axial temperature profiles measured within the monolith for feed concentrations between 500 and 10,000 ppm. Results presented in this figure correspond to data recorded at 290°C for conversions greater than about 75%. For the 500 ppm challenge, the recorded temperatures deviated by less than 2°C from the average (of the five thermocouples) at all points within the monolith, indicating that near isothermal operation had been achieved. Upon increasing the feed concentration to 10,000 ppm, the deviation in the axial temperature measurements became more pronounced, especially near the entrance to the monolith. Note that the air inlet temperature is about 10°C less than the average temperature of the catalyst.

Because of the activity of hydrogen cyanide and the difficulty in controlling the catalyst temperature, great difficult was encountered in attempting to maintain the catalyst isothermal. Attempts to operate the catalyst at temperatures greater than 290°C were mostly unsuccessful, since the heat generated by the chemical reaction could not be removed fast enough to prevent the reaction from running away; i.e. going to complete conversion. As a result, reaction temperatures below 290°C were investigated, with a minimal amount of data reported at 310°C.

Reaction rate data were recorded at temperatures of 200, 230, 260, 290 and 310° C for concentrations between 500 and 20,000 ppm (602 and 24,080 mg/m^3) at 6±1 psig in dry air. Figures 7 through 11 report the conversion of hydrogen cyanide as a function of residence time at reaction temperatures of 200, 230, 265, 290 and 310°C, respectively. Results presented in these figures show that increasing the concentration of hydrogen cyanide has a significant effect on conversion. For example, doubling the feed concentration of hydrogen cyanide from 5,000 ppm to 10,000 ppm at 290°C at a residence time of 0.3 seconds results in the conversion decreasing from near 100% to about 15%. Residence time was also found to have a significant effect on the conversion of hydrogen cyanide. For conversions greater than about 30%, slight changes in the residence time caused the conversion to increase to nearly 100%. For example, at 290°C, increasing the residence time of a 5,000 ppm feed from 0.2 to 0.3 seconds results in the conversion increasing from about 40% to over 95%.

The solid lines in the Figures 7 through 11 represent the data correlated using the mathematical model. Results show that while the model may not always accurately predict the conversion of hydrogen cyanide, the model accurately predicts the residence time required to achieve the stated conversion.

An additional set of experiments was performed to evaluate the model's ability to predict data recorded at elevated pressures. Figure 12 reports the conversion of 5,000 ppm (6,025 mg/m^3) hydrogen cyanide as a function of residence time under total pressures of 6, 15 and 23 psig. Data presented in this figure were recorded at 290°C. Results demonstrate that the total pressure has no effect, to within experimental error, on the conversion of hydrogen cyanide. This result is consistent with that predicted by the mathematical model.
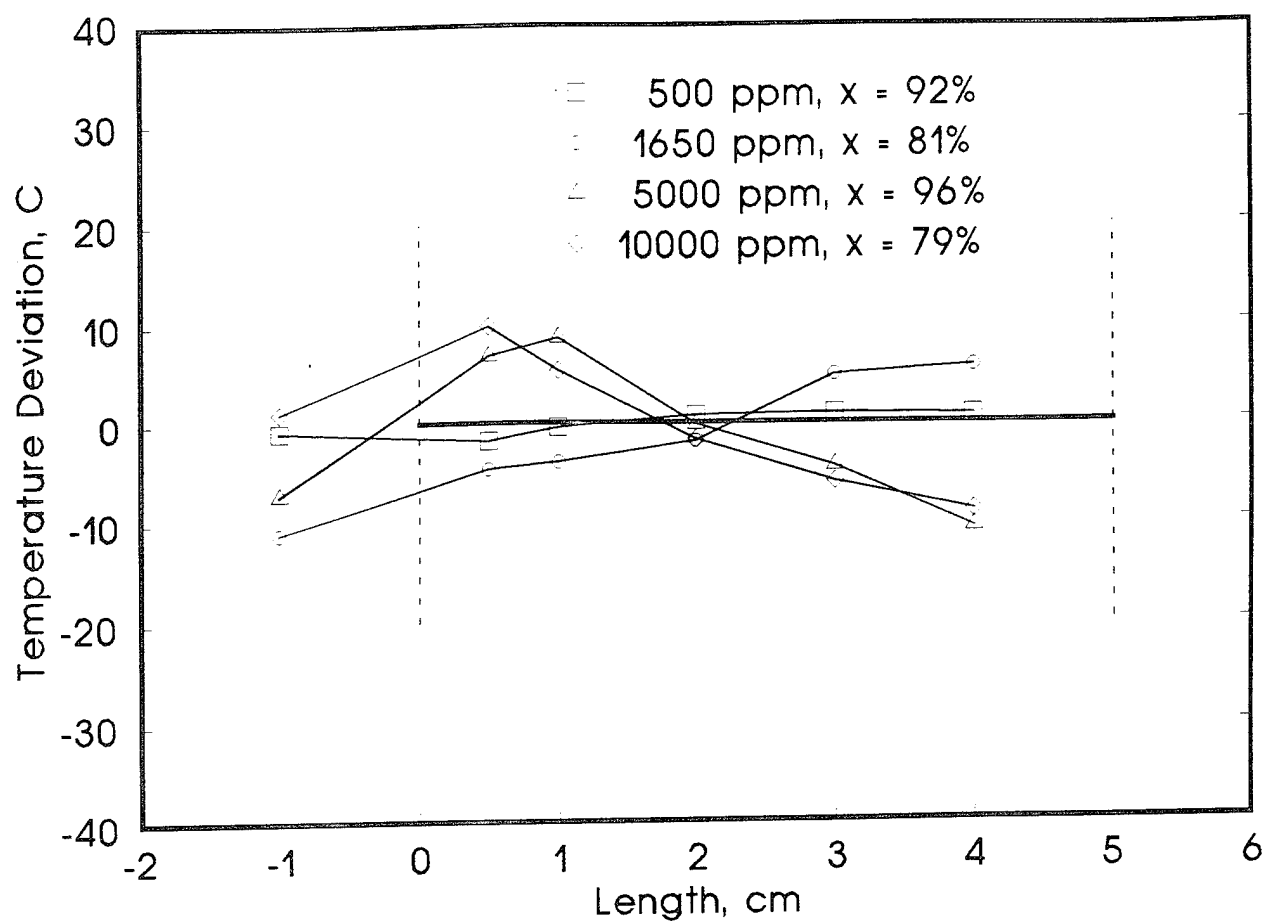
Figure 6: Axial Temperature Profiles Recorded During the Isothermal Oxidation of Hydrogen Cyanide at 290°C.
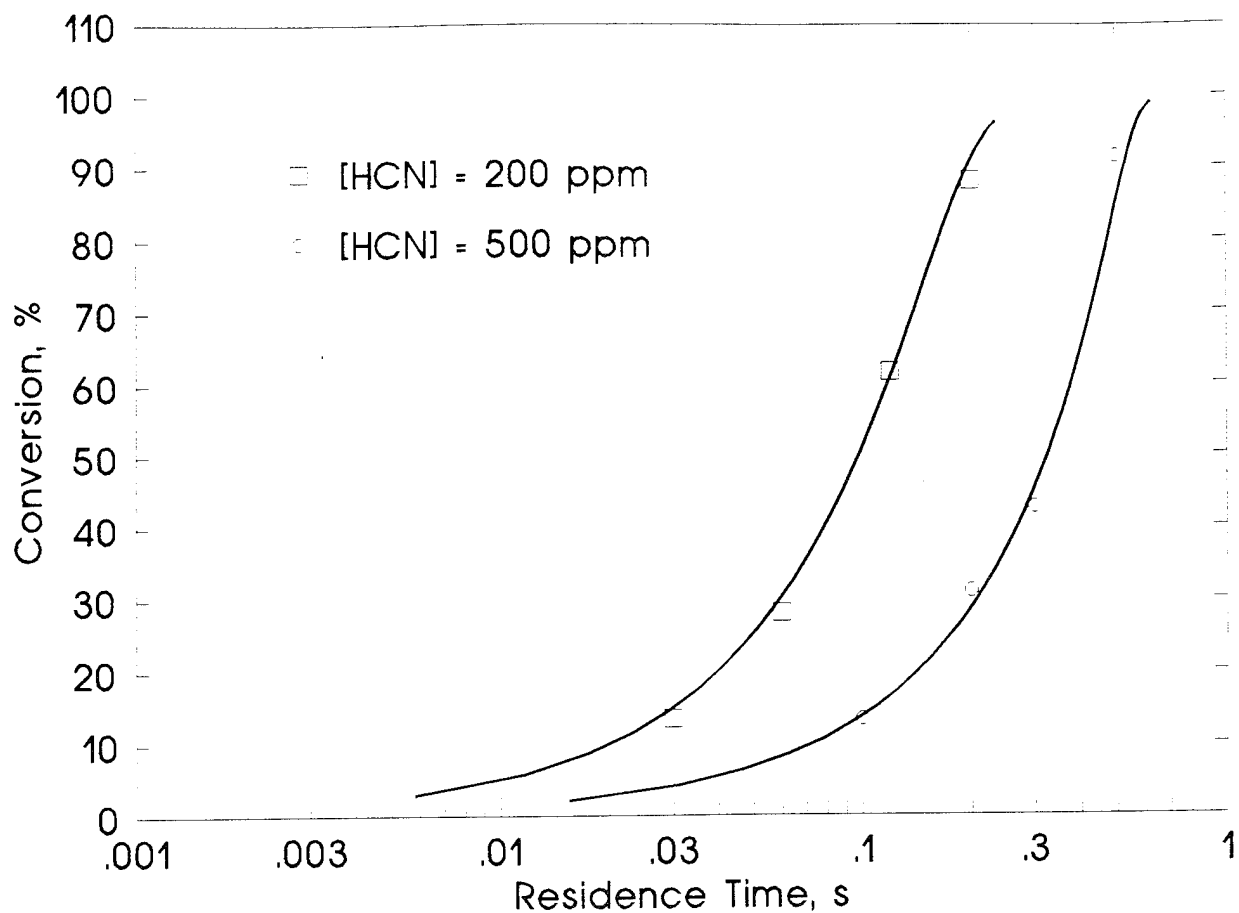
Figure 7: Conversion as a Function of Residence Time for the Oxidation of Hydrogen Cyanide at 200°C. The solid lines in the figure represent data correlated using the mathematical model.
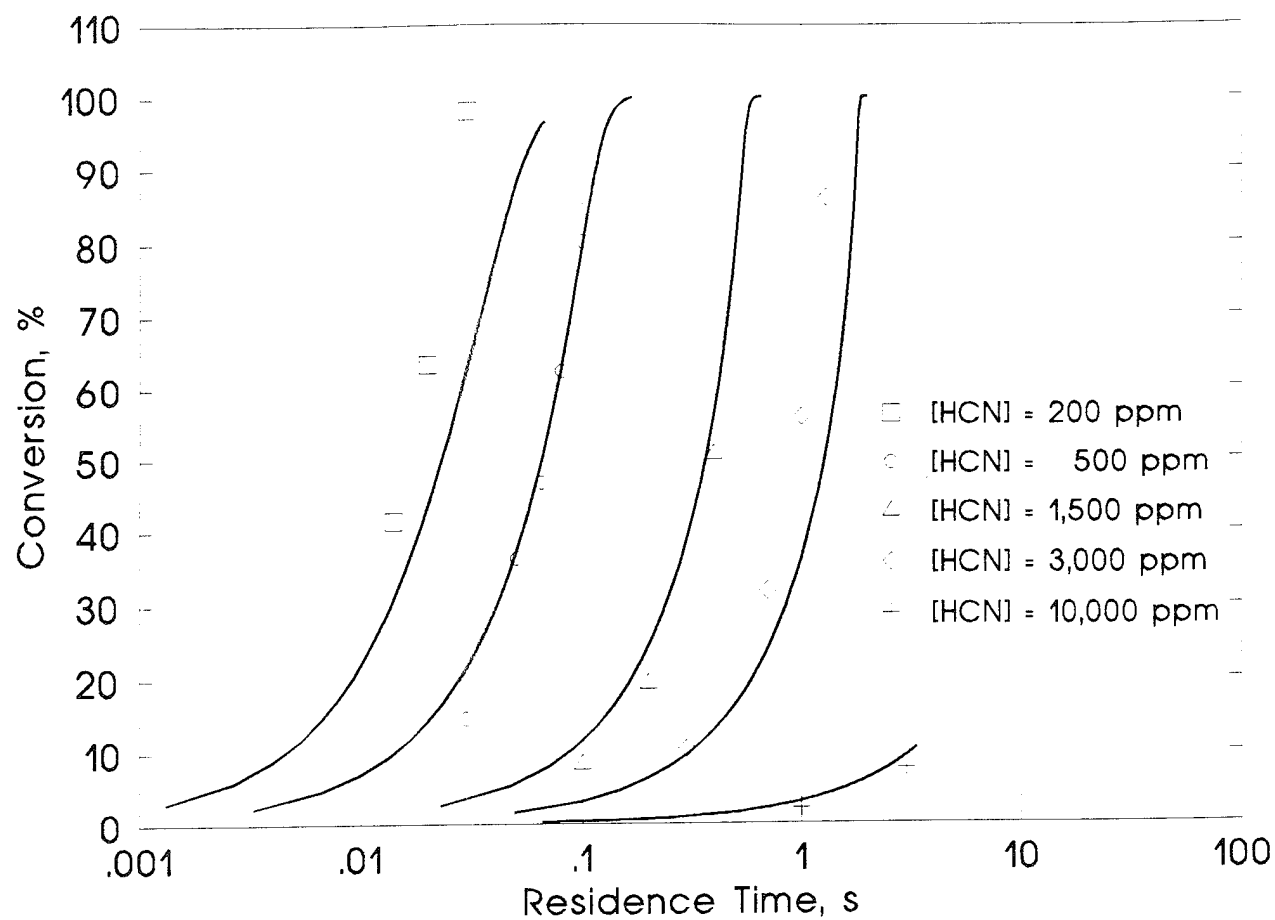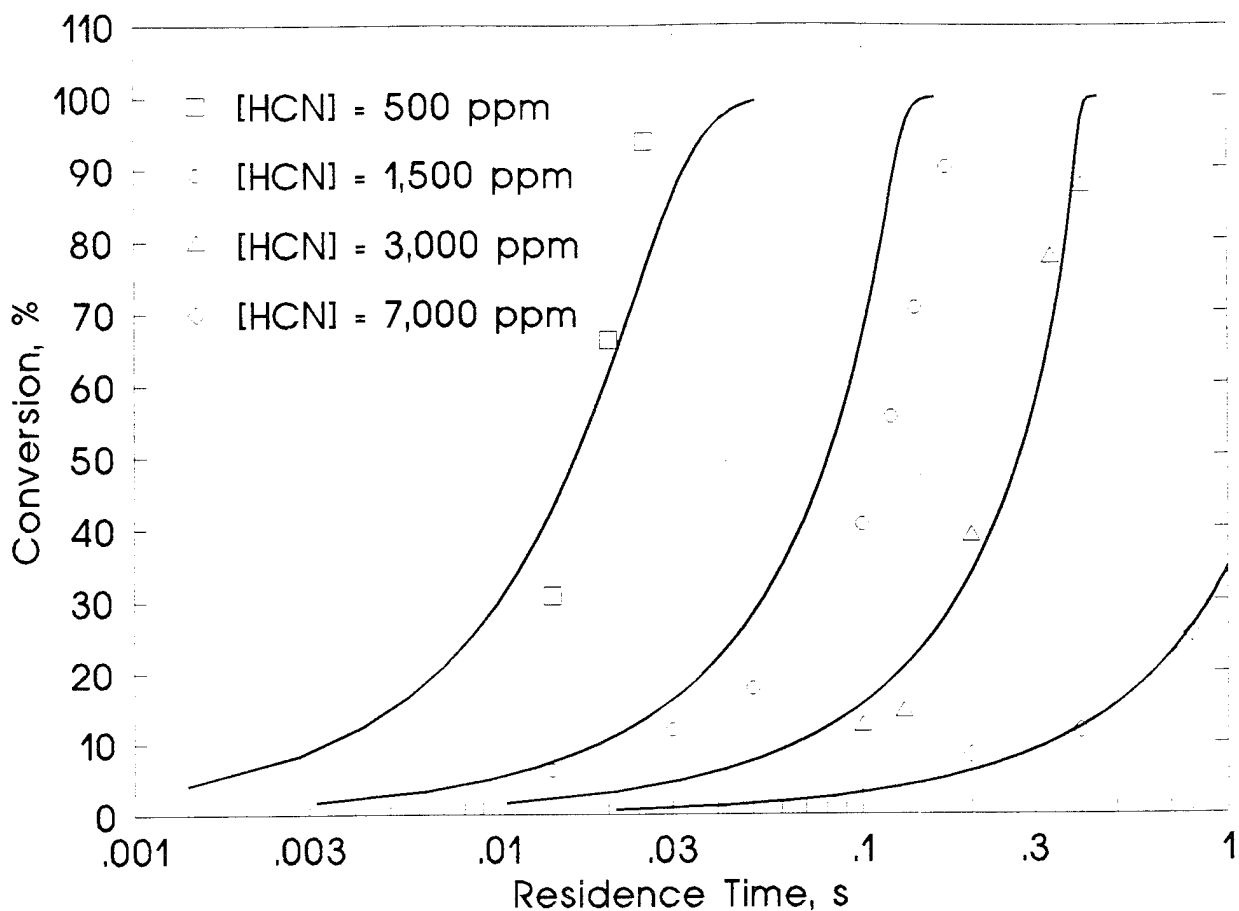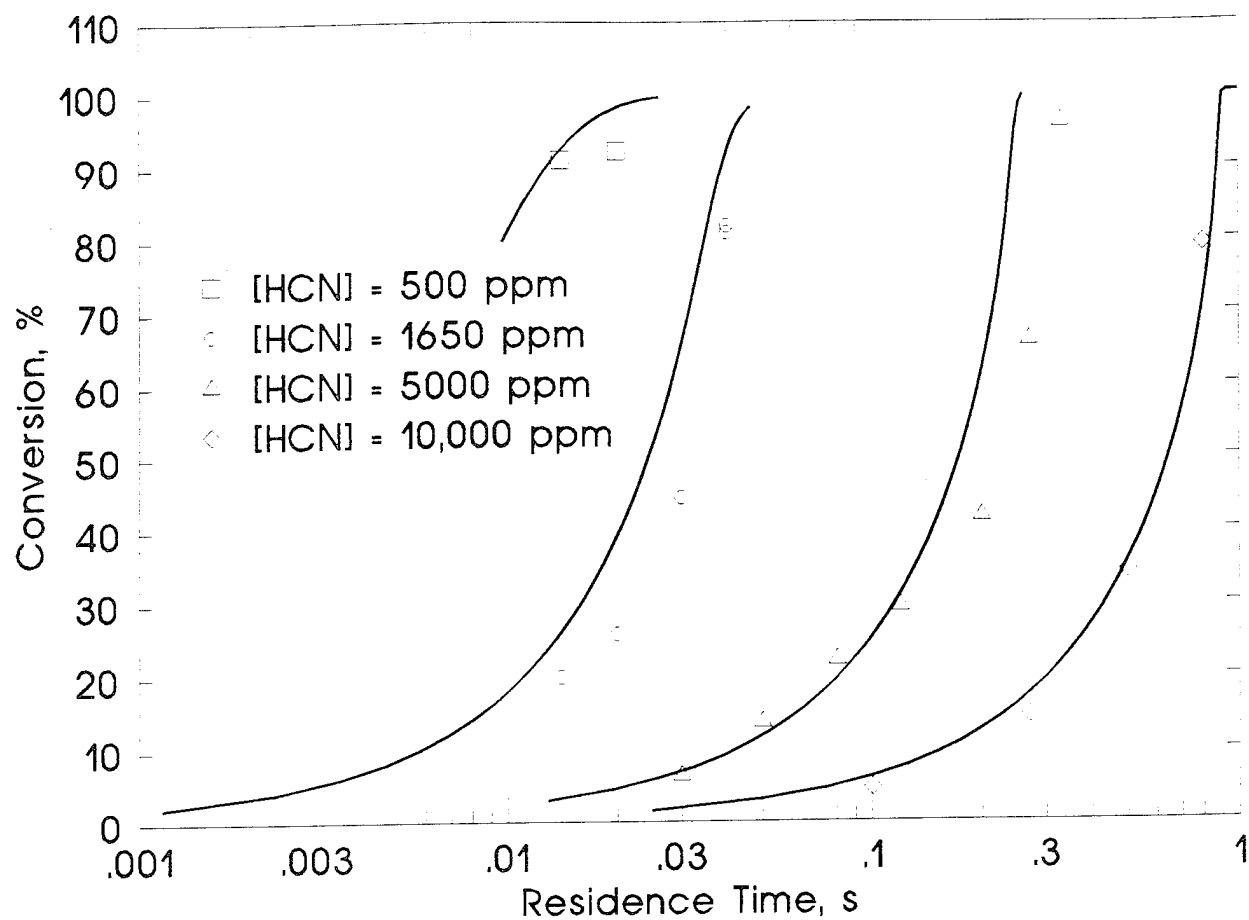
Figure 8: Conversion as a Function of Residence Time for the Oxidation of Hydrogen Cyanide at 230°C. The solid lines in the figure represent data correlated using the mathematical model.
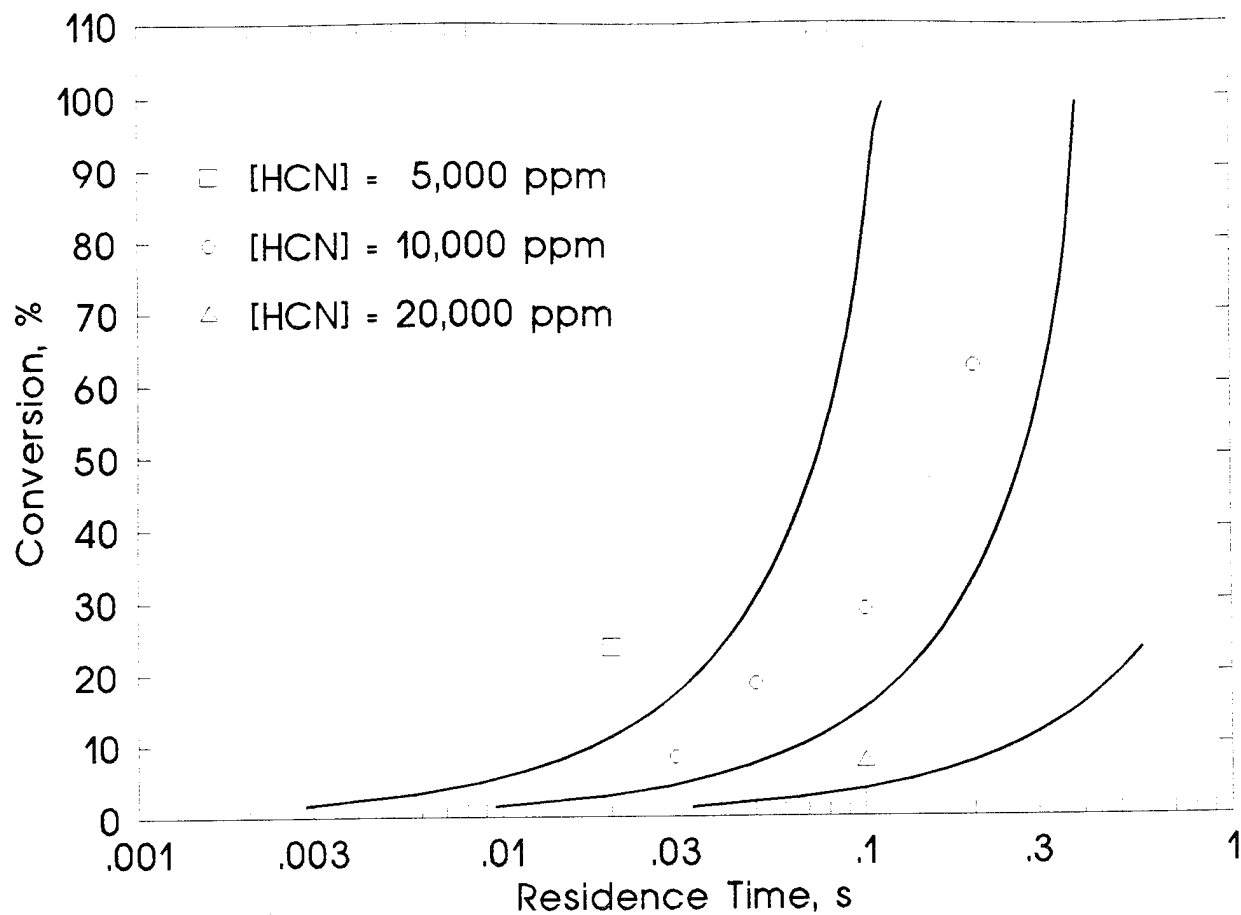
Figure 9: Conversion as a Function of Residence Time for the Oxidation of Hydrogen Cyanide at 260°C. The solid lines in the figure represent data correlated using the mathematical model.
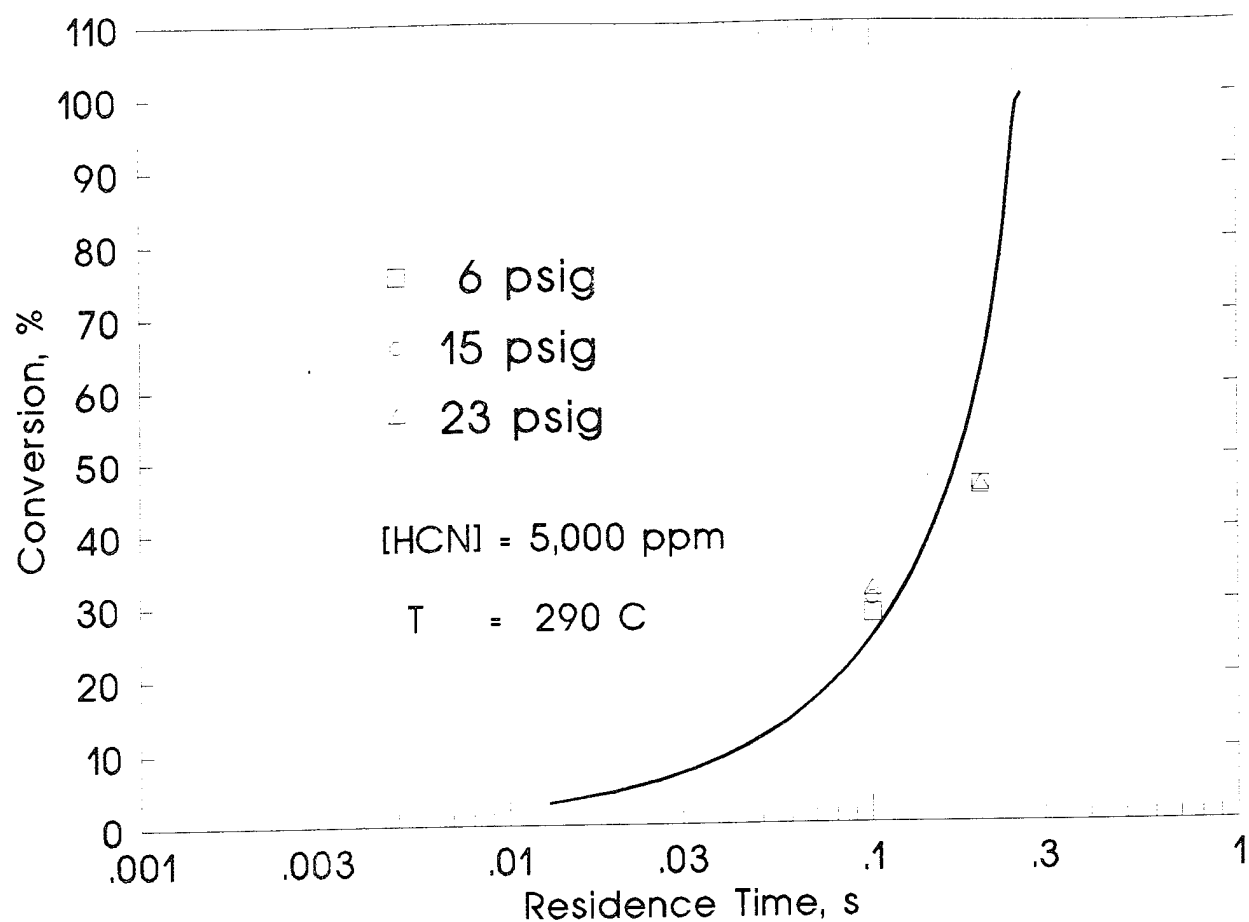
Figure 10: Conversion as a Function of Residence Time for the Oxidation of Hydrogen Cyanide at 290°C. The solid lines in the figure represent data correlated using the mathematical model.

Figure 11: Conversion as a Function of Residence Time for the Oxidation of Hydrogen Cyanide at 310°C. The solid lines in the figure represent data correlated using the mathematical model.

Figure 12: Effects of Total Pressure on the Conversion of Hydrogen Cyanide as a Function of Residence Time at 290°C. The solid lines in the figure represent data correlated using the mathematical model.

Equation 8 reports the reaction rate expression for the oxidation of hydrogen cyanide derived from the Langmuir-Hinshelwood assumptions. If hydrogen cyanide is strongly adsorbed onto the catalyst surface (high hydrogen cyanide concentrations), the reaction rate expression reduces to:

$$Rate = \frac{kK_{O_2}C_{O_2}}{K_{HCN}C_{HCN}} \qquad (21)$$

In this case, increasing the total pressure will result in a similar increase in the concentration of hydrogen cyanide and oxygen, and the effects will cancel out. On the other hand, if oxygen is strongly adsorbed onto the catalyst surface (low hydrogen cyanide concentrations), the rate expression reduces to:

$$Rate = \frac{kK_{HCN}C_{HCN}}{K_{O_2}C_{O_2}} \qquad (22)$$

Again, increasing the total pressure will increase both the hydrogen cyanide and oxygen concentration, with the effects canceling out. In either case, increasing the total pressure is not expected to affect the reaction rate and hence conversion of hydrogen cyanide.

A summary of the raw data presented in this section is provided in Appendix A.

Transient Rate Measurements: Transient reaction rate measurements were recorded for the purpose of evaluating the catalyst's performance against challenges which might be encountered during battlefield conditions. As described in the NDRC Report[2], during a chemical attack, the ambient agent concentration will increase in a manner very nearly resembling a step change. When a catalyst is confronted with a rapid change in concentration, such as during a chemical attack, a catalyst would be expected to behave as follows: At the on-set of the chemical attack, the temperature of the catalyst bed will begin to rise, ultimately approaching its adiabatic value. The increase in the catalyst temperature will be accompanied by a corresponding decrease in the effluent concentration of agent. However, should the rate at which the catalyst temperature increase be slow relative to the duration of the chemical attack, then the design of the reactor cannot take advantage of the heat generated by the chemical reaction. Otherwise, a significant dose of chemical agent may elute through the catalyst. On the other hand, should the rate at which the catalyst temperature increases be fast relative to the duration of the chemical attack, then the design of the reactor can take advantage of the heat generated by the chemical reaction. Should this be the case, the catalyst will be able to operate at a lower temperature, thereby reducing the energy requirements of the system.

The chemical attack scenario observed by Latimer[2] was simulated under laboratory conditions by exposing the catalyst to a pulse of hydrogen cyanide, with the duration of the pulse being three minutes. Feed concentrations between 5,000 and 27,500 ppm (6,025 and 33,135 mg/m^3) were employed at air inlet temperatures of 290, 310 and

31

330°C at residence times of 0.33 seconds. All data are reported for runs conducted under a total pressure of 6.0 psig. Figures 13 through 15 illustrate the behavior of the catalyst resulting from exposure to a 5,000 ppm (6,000 mg/m^3) step change in concentration at an air inlet temperature of 294°C and residence times of 0.25, 0.33 and 0.50 seconds, respectively. For these runs, the effluent concentration was at or near the detection limit of the mass selective detector. Upon exposure of the catalyst to the challenge, the catalyst temperature rises rapidly, especially near the inlet. This behavior indicates that the majority of hydrogen cyanide is consumed near the inlet of the monolith core. As time goes on, the outlet temperature begins to rise as a result of heat transfer from the gas phase in the axial direction. One effect of increasing the residence time, as evident from the data presented in Figures 13 through 15, is to decrease the rate at which the air outlet temperature increases. Increasing the residence time from 0.25 seconds to 0.5 seconds, results in decreasing the air outlet temperature at the end of the challenge from about 340° C to less than 300°C.

Effects of Feed Concentration: Figures 14, 16 and 17 report the feed and effluent concentration of hydrogen cyanide as a function of time (with time = zero being defined as the initiation of the pulse), as well as the axial catalyst temperature profiles recorded near the center of the catalyst at discrete times during the challenge for runs conducted with an air inlet temperature of 293°C at a residence time of 0.33 seconds. Data presented in these figures correspond to feed concentrations of 5,000, 7,500 and 10,000 ppm, respectively. For the 5,000 ppm challenge (Figure 14), virtually no hydrogen cyanide was detected in the effluent stream. The catalyst temperature increases 96°C at the hottest spot, which is consistent with the expected adiabatic temperature rise. Upon increasing the effluent concentration to 7,500 ppm (Figure 16), hydrogen cyanide is present in the effluent stream, with the concentration decreasing sharply with time. The rapid decrease is a result of heat generated by the reaction being accumulated within the monolith and hence increasing the reaction rate. For this run, 99.4% of the hydrogen cyanide was removed by the catalyst during the challenge. Upon increasing the feed concentration to 10,000 ppm, greater quantities of hydrogen cyanide are present in the effluent stream, and the transient effects become more apparent. The effluent concentration decreases by nearly two orders of magnitude over the duration of the challenge as a result of the catalyst temperature increasing by 170°C.

Results of the isothermal reaction rate study showed the oxidation of hydrogen cyanide to be very sensitive to concentration. This behavior becomes obvious looking at the transient rate data reported in Figures 18 through 20. Data presented in these figures correspond to data collected with an air inlet temperature of 315°C. For a feed concentration of 10,000 ppm (12,000 mg/m^3, Figure 18), the maximum effluent concentration was about 300 ppm, and 99.90% of the hydrogen cyanide was oxidized during the challenge. Increasing the feed concentration to 15,000 ppm (18,000 mg/m^3, Figure 19), results in the catalyst lighting-off more slowly. Following 30 seconds into the run, the maximum catalyst temperature has increased only 30°C, compared to 120°C for the previous run. Further, the maximum effluent concentration of hydrogen cyanide is
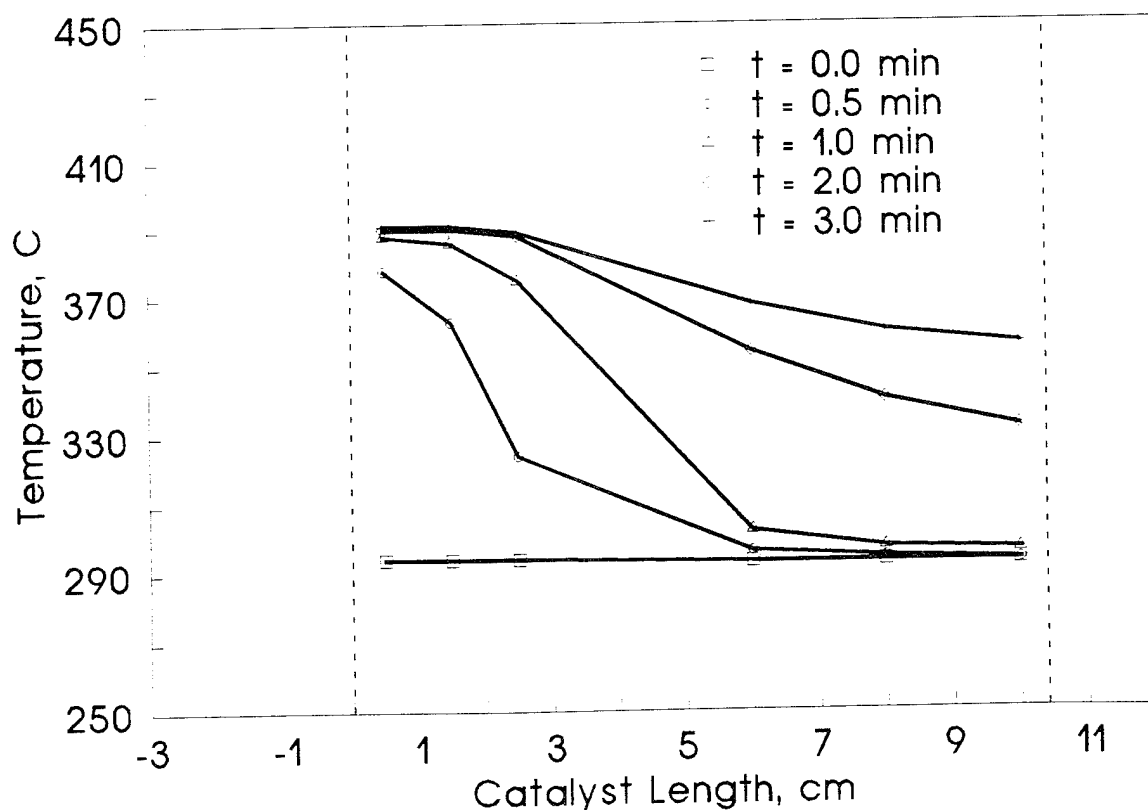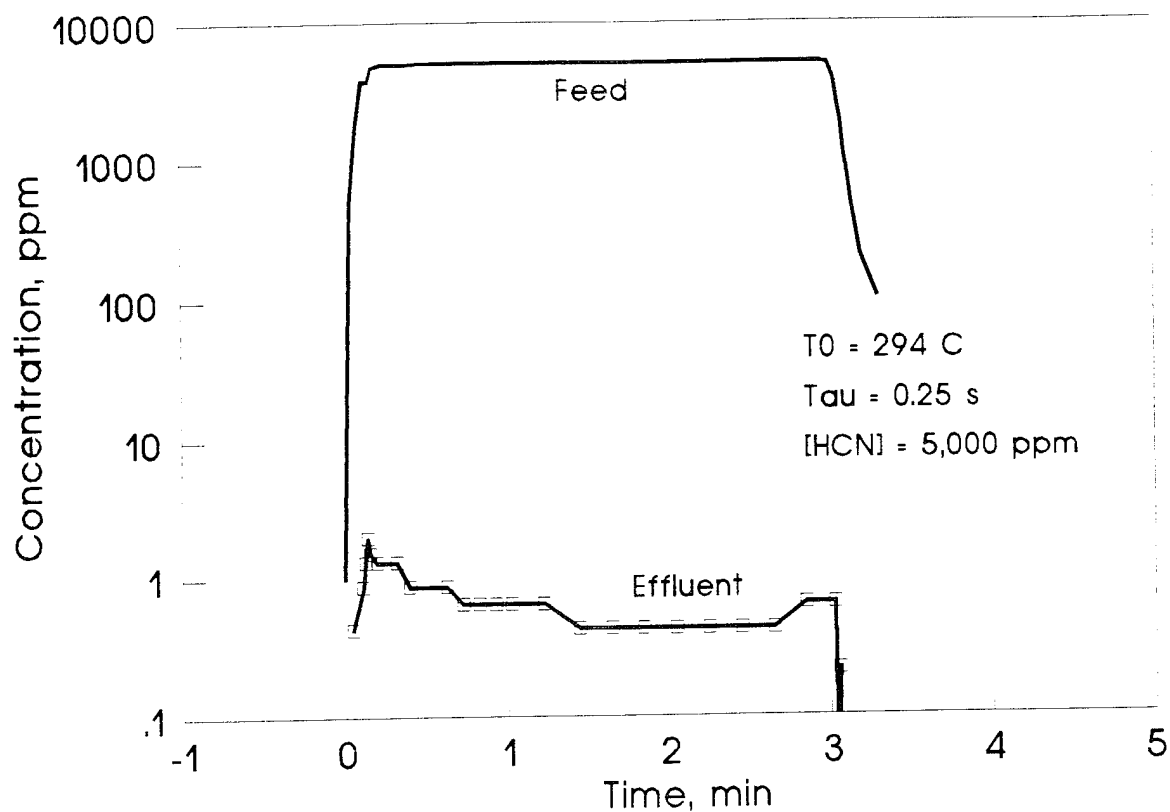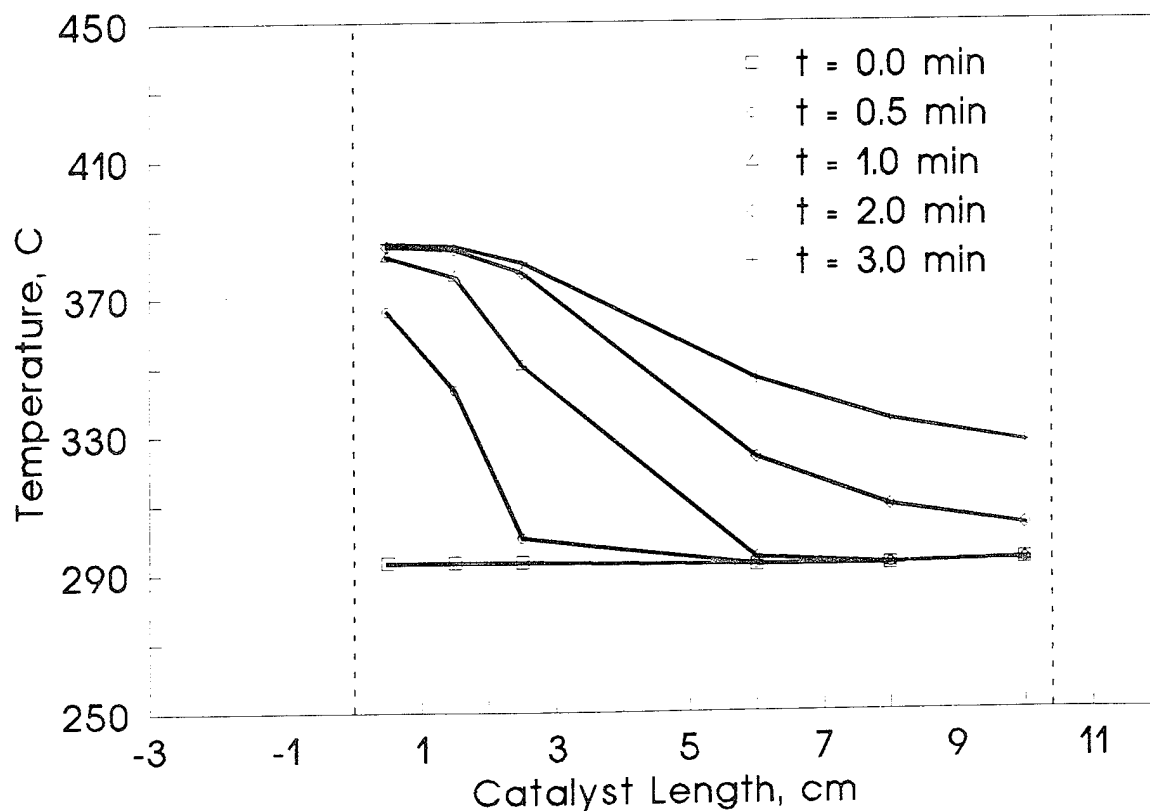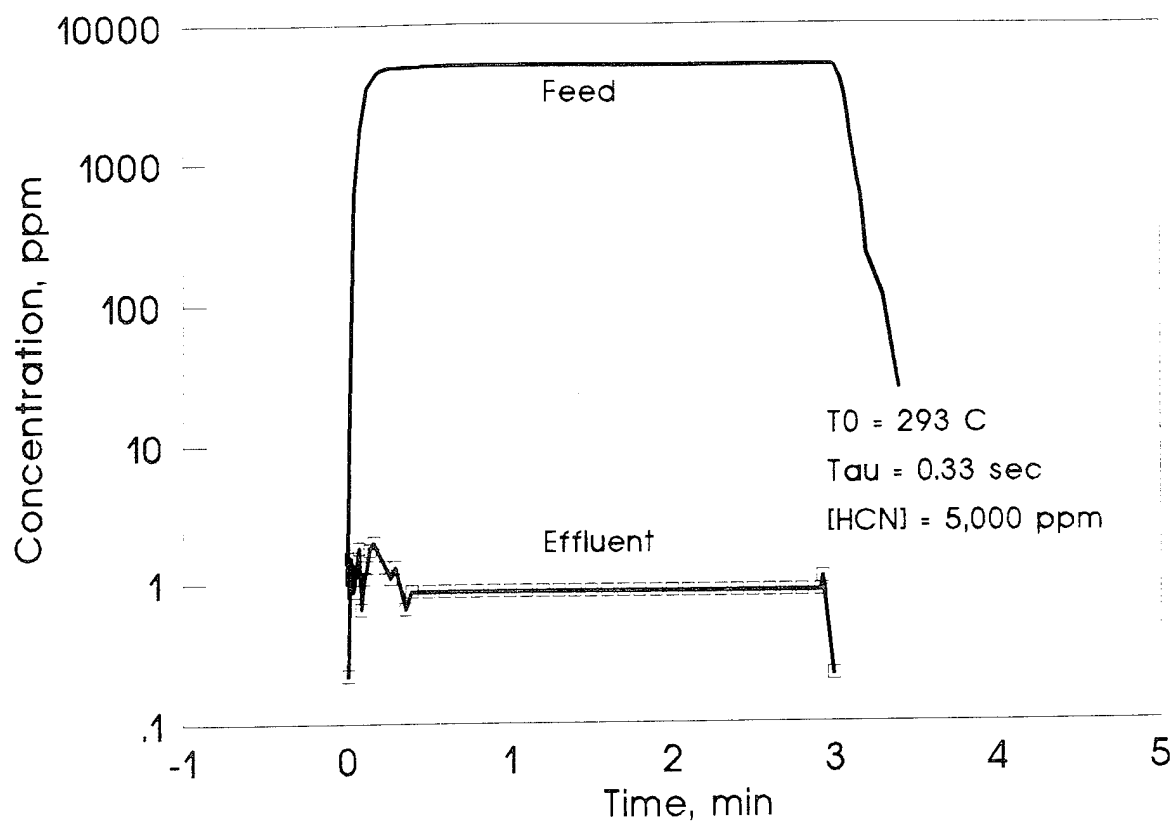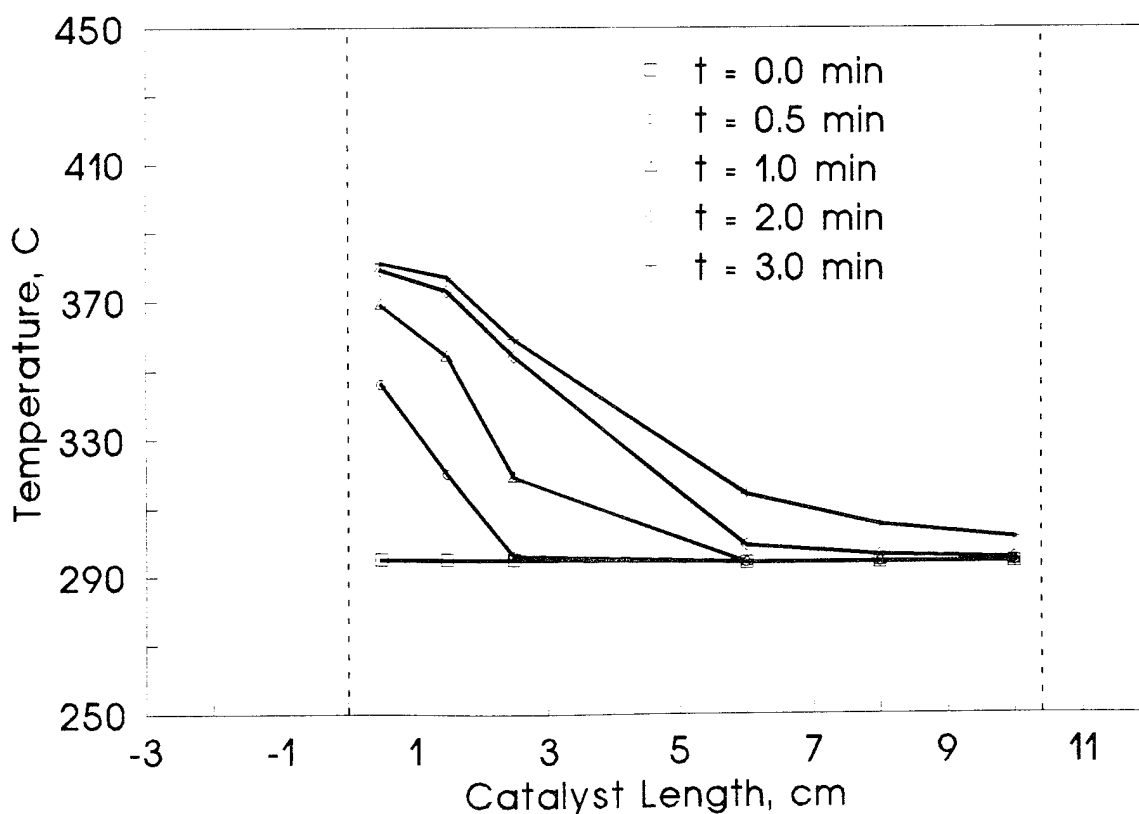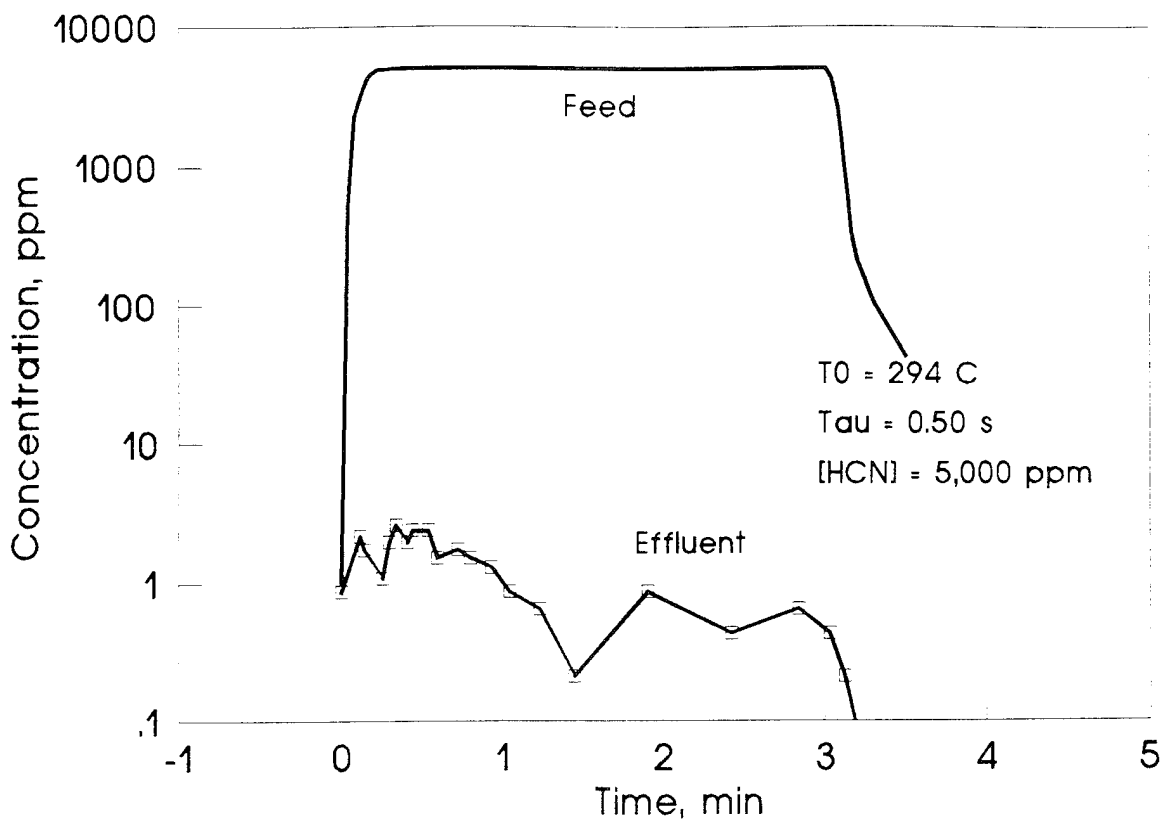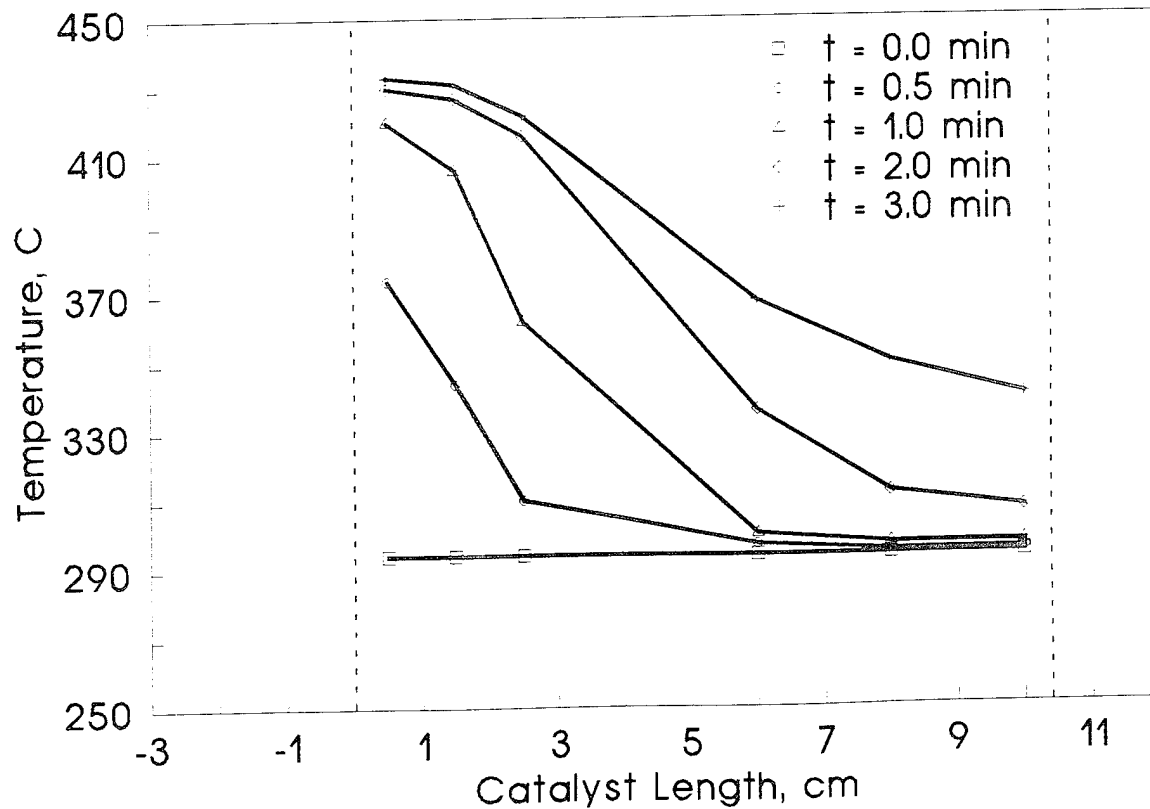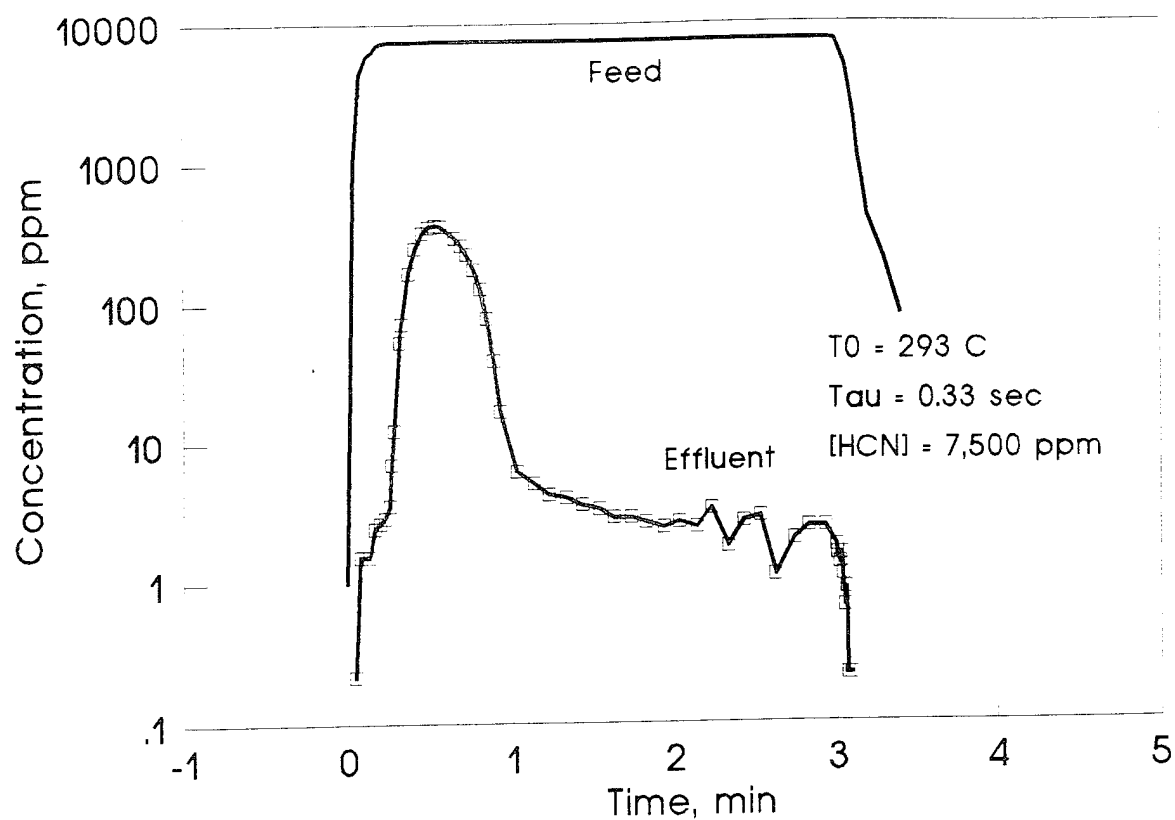
Figure 13: Feed and Effluent Concentration of Hydrogen Cyanide as a Function of Time (Top) and Catalyst Temperature Profile at Discrete Times (Bottom) Recorded During a Pulse Challenge of Hydrogen Cyanide. Temperature = 294°C, [HCN] = 5,000 ppm, τ = 0.25 s.

33

Figure 14: Feed and Effluent Concentration of Hydrogen Cyanide as a Function of Time (Top) and Catalyst Temperature Profile at Discrete Times (Bottom) Recorded During a Pulse Challenge of Hydrogen Cyanide. Temperature = 294°C, [HCN] = 5,000 ppm, τ = 0.33 s.
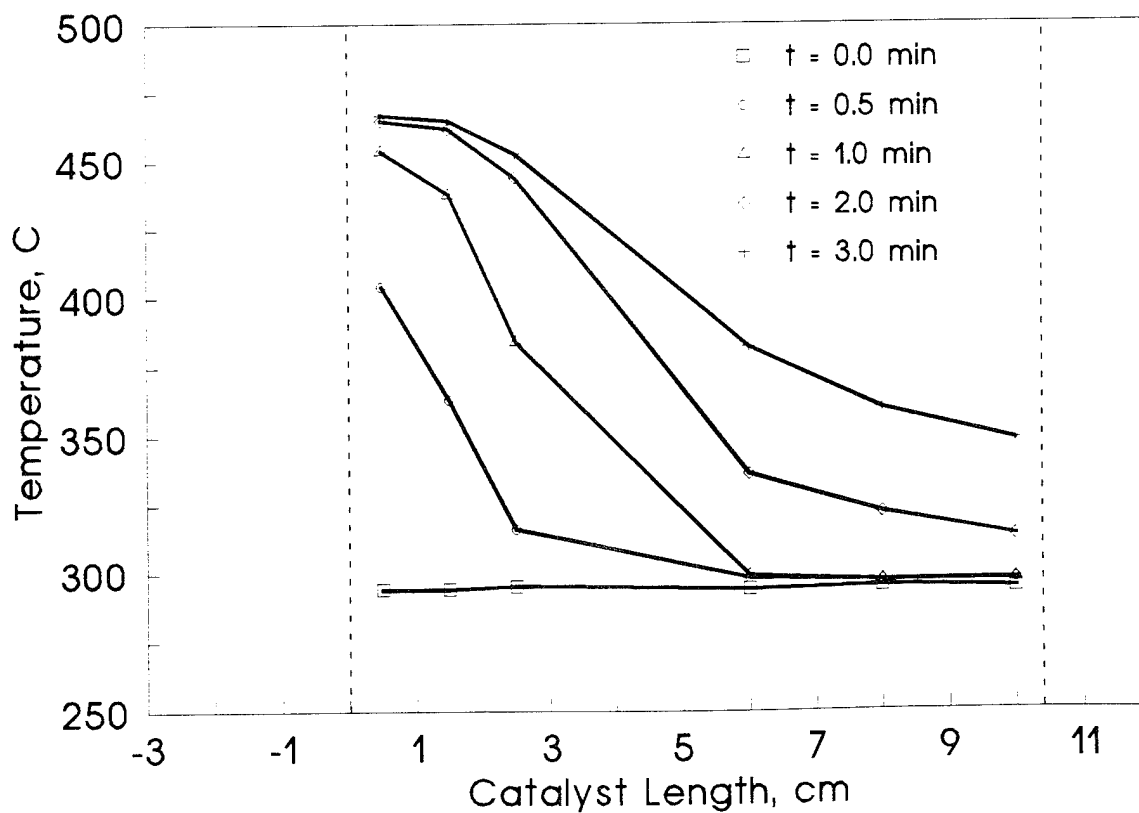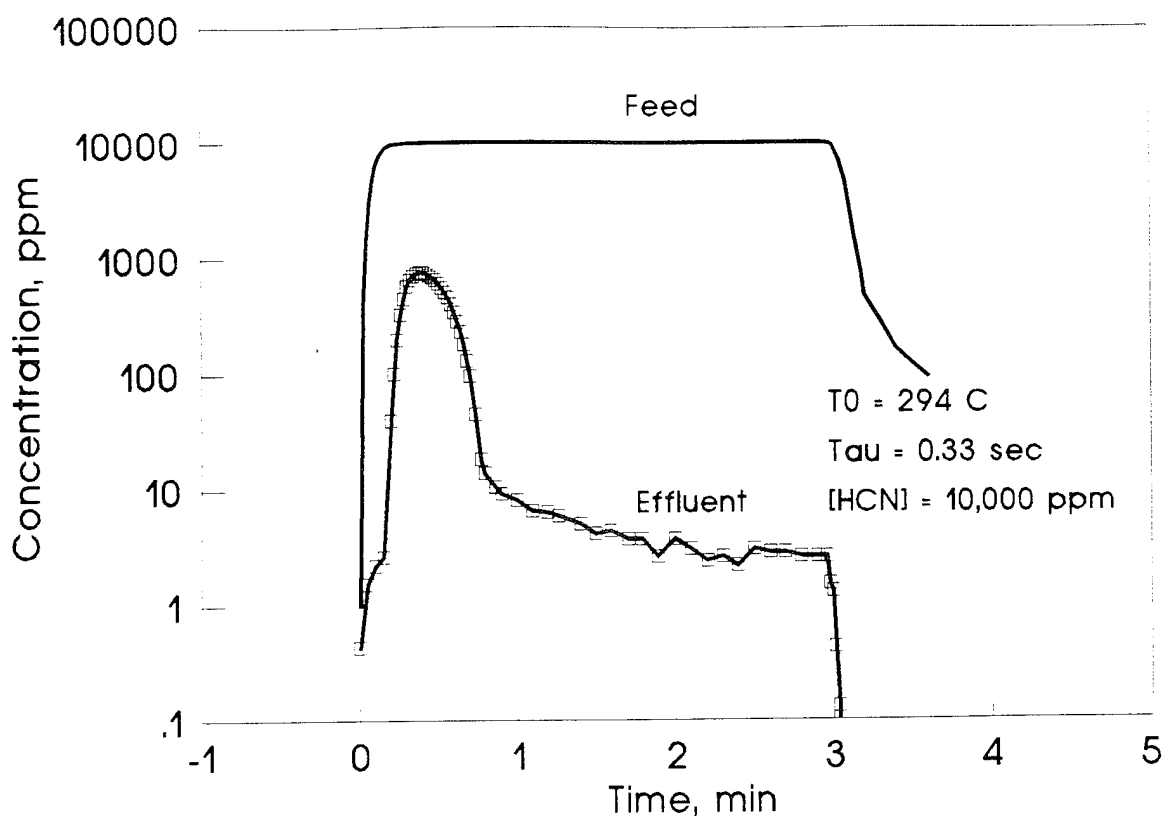
34

Figure 15: Feed and Effluent Concentration of Hydrogen Cyanide as a Function of Time (Top) and Catalyst Temperature Profile at Discrete Times (Bottom) Recorded During a Pulse Challenge of Hydrogen Cyanide. Temperature = 294°C, [HCN] = 5,000 ppm, τ = 0.50 s.

35

Figure 16: Feed and Effluent Concentration of Hydrogen Cyanide as a Function of Time (Top) and Catalyst Temperature Profile at Discrete Times (Bottom) Recorded During a Pulse Challenge of Hydrogen Cyanide. Temperature = 293°C, [HCN] = 7,500 ppm, τ = 0.33 s.
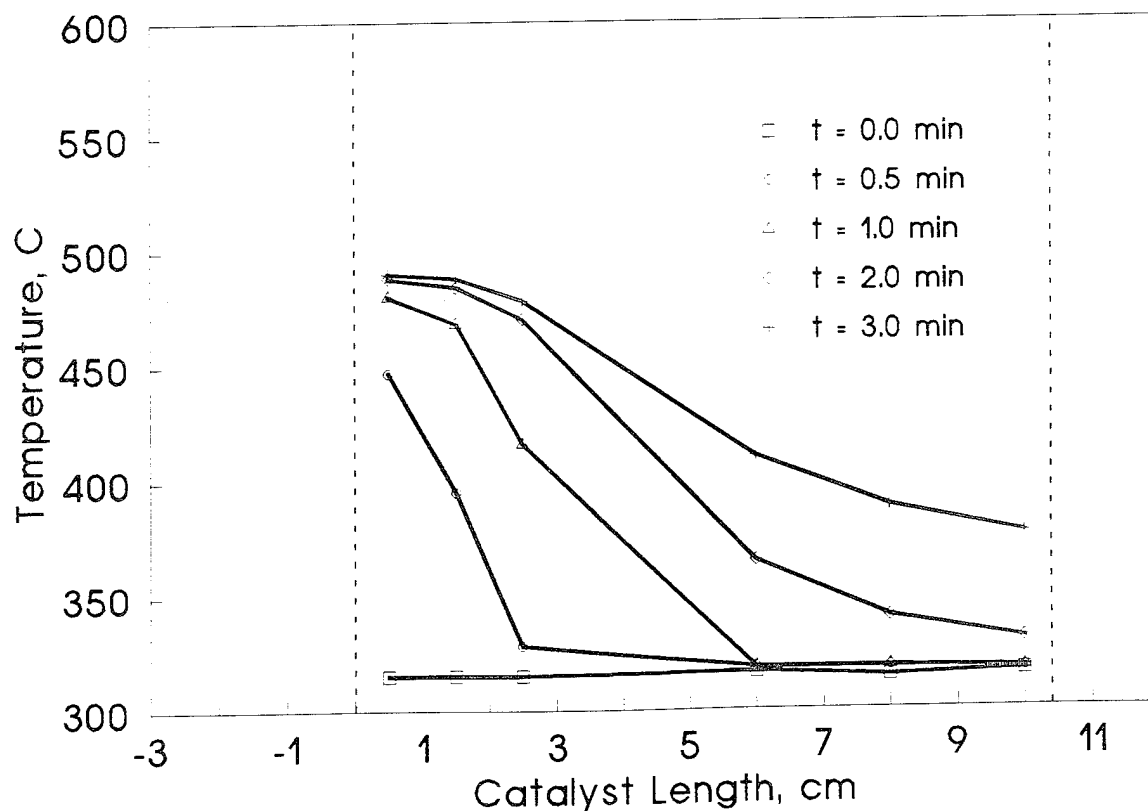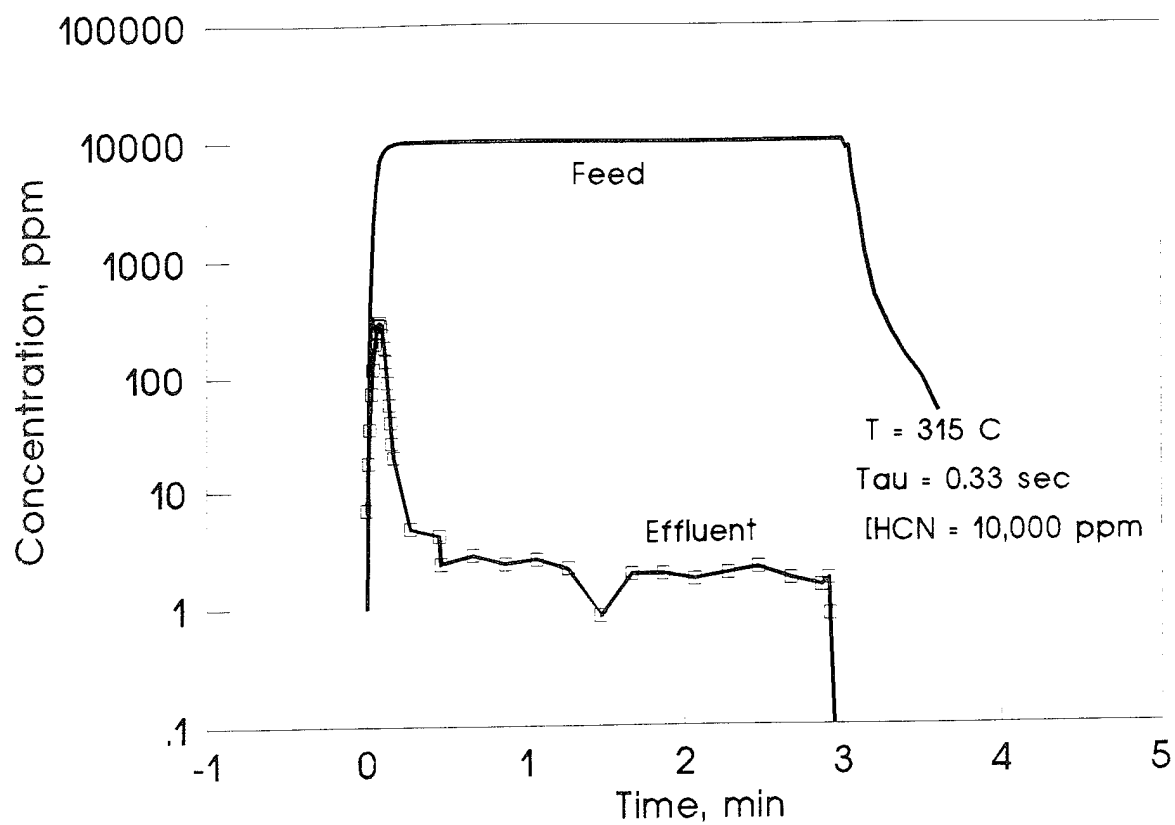
36

Figure 17: Feed and Effluent Concentration of Hydrogen Cyanide as a Function of Time (Top) and Catalyst Temperature Profile at Discrete Times (Bottom) Recorded During a Pulse Challenge of Hydrogen Cyanide. Temperature = 294°C, [HCN] = 10,000 ppm, τ = 0.33 s.

37

Figure 18: Feed and Effluent Concentration of Hydrogen Cyanide as a Function of Time (Top) and Catalyst Temperature Profile at Discrete Times (Bottom) Recorded During a Pulse Challenge of Hydrogen Cyanide. Temperature = 315°C, [HCN] = 10,000 ppm, τ = 0.33 s.
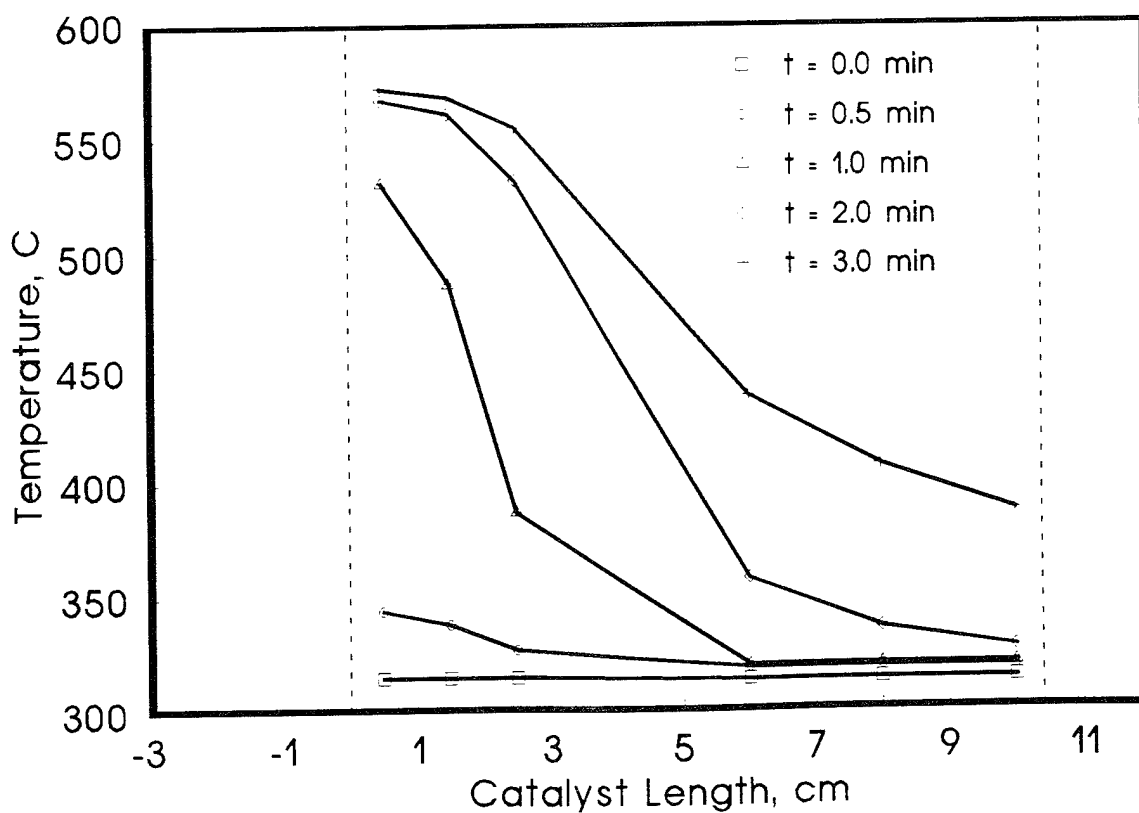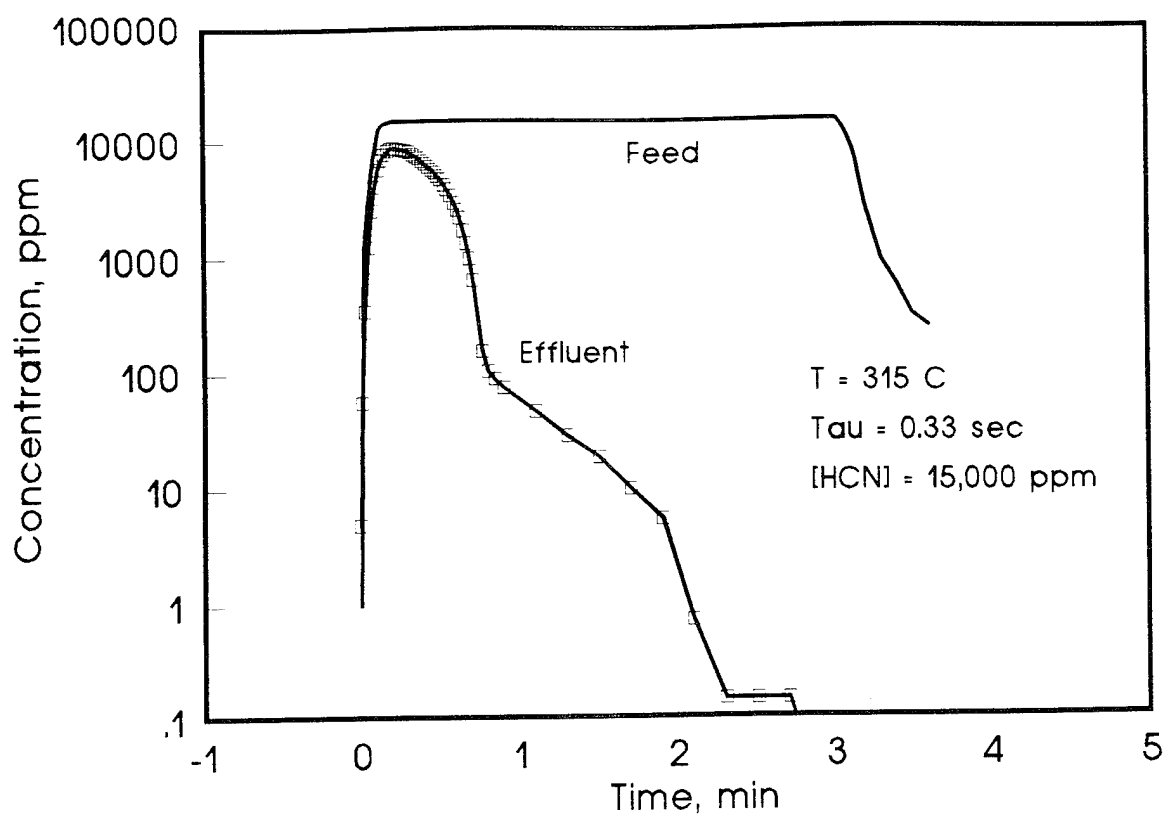
38

Figure 19: Feed and Effluent Concentration of Hydrogen Cyanide as a Function of Time (Top) and Catalyst Temperature Profile at Discrete Times (Bottom) Recorded During a Pulse Challenge of Hydrogen Cyanide. Temperature = 315°C, [HCN] = 15,000 ppm, τ = 0.33 s.
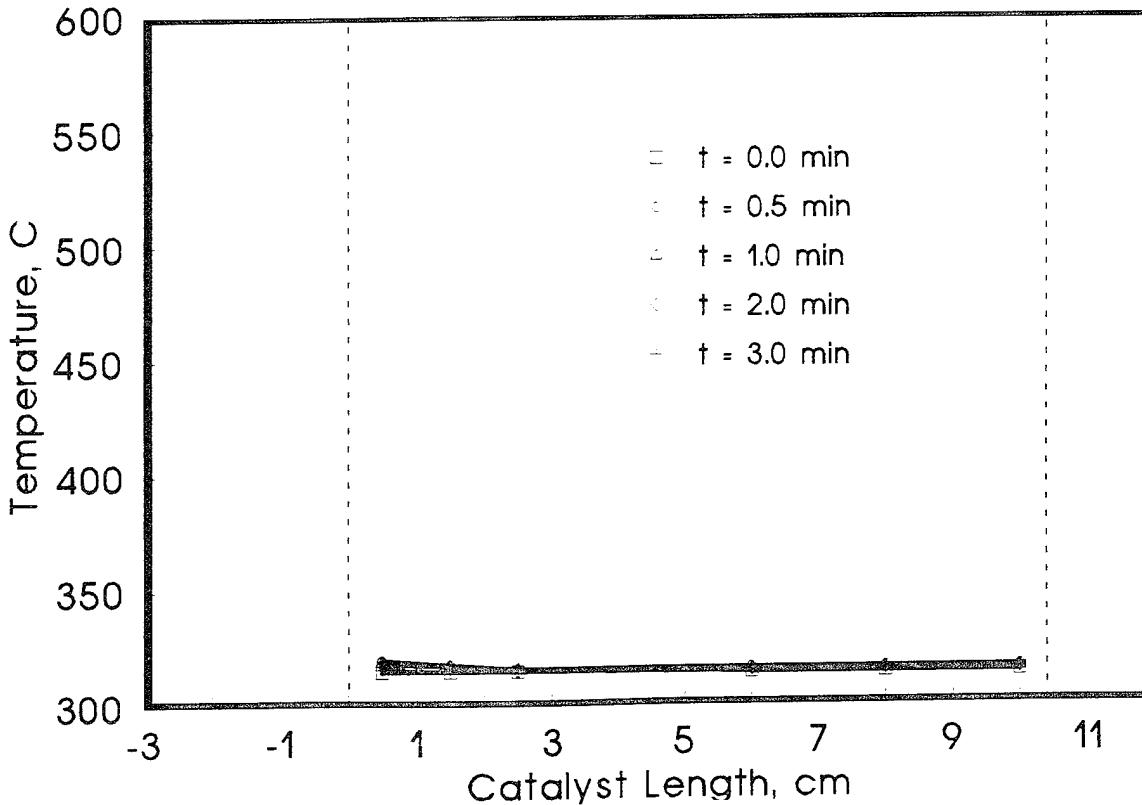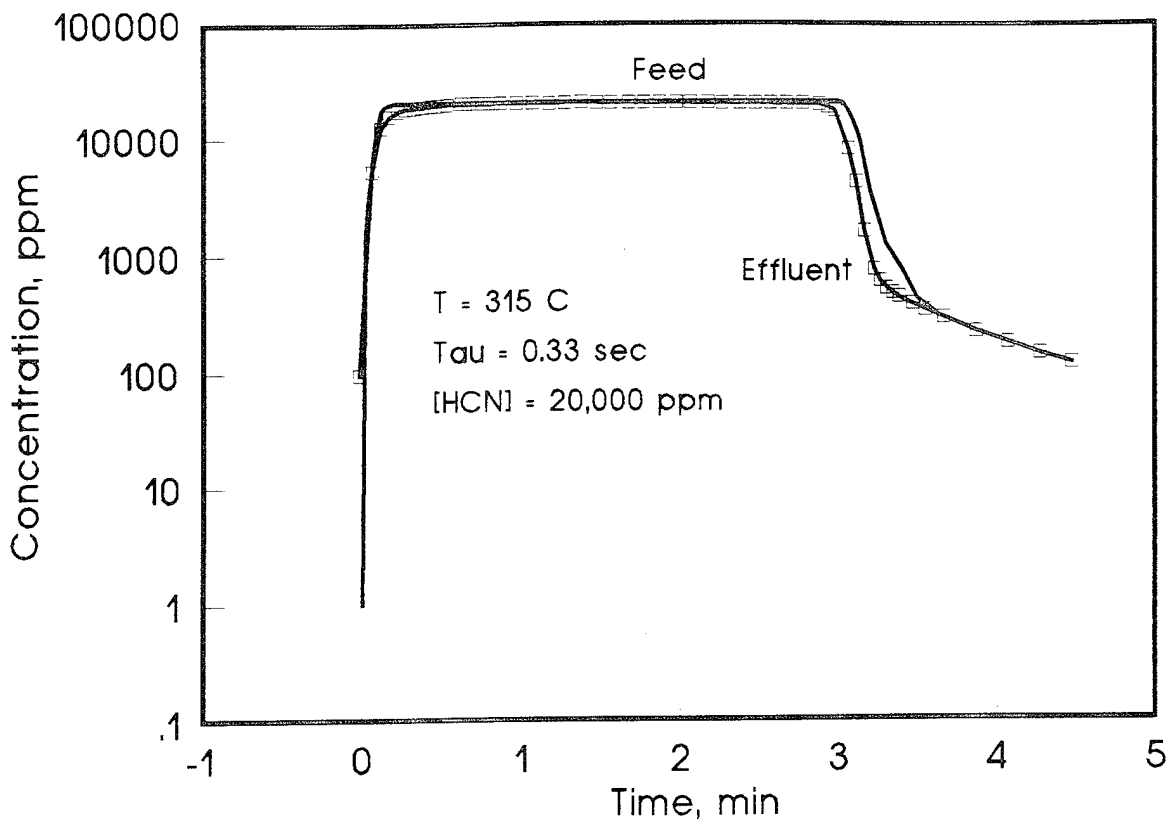
39

Figure 20: Feed and Effluent Concentration of Hydrogen Cyanide as a Function of Time (Top) and Catalyst Temperature Profile at Discrete Times (Bottom) Recorded During a Pulse Challenge of Hydrogen Cyanide. Temperature = 315°C, [HCN] = 20,000 ppm, τ = 0.33 s.

8,800 ppm (conversion only 12%). However, following 30 seconds, the catalyst lights-off, and the effluent concentration decreases sharply throughout the remainder of the run. In this case, only 91.3% of the hydrogen cyanide in the feed was reduced during the challenge. Increasing the feed concentration further (Figure 20) to 20,000 ppm (24,000 mg/m^3), results in the catalyst surface being smothered by hydrogen cyanide and hence virtually no reaction has taken place. For this run, the air inlet temperature was insufficient to cause the catalyst to light-off.

Increasing the air inlet temperature to 331°C significantly improved the catalytic activity. These results are reported in Figures 21 through 23 for feed concentrations of 10,000, 20,000 and 27,500 ppm (12,000, 24,000 and 33,000 mg/m^3) at a residence time of 0.33 seconds. Results show that only for the highest feed concentration was a significant quantity of hydrogen cyanide observed in the effluent (Figure 23). In this case, the dose reduction of hydrogen cyanide during the challenge was 99.97%.

Effects of Air Inlet Temperature: Changes in the air inlet temperature were found to have the greatest impact on the transient properties of the catalyst. Increasing the air inlet temperature from 290 to 330°C for a residence time of 0.33 seconds and a feed concentration of 10,000 ppm (Figures 17, 18 and 21) results in greatly enhancing the transient properties of the catalyst. The initial effluent concentration is greatly decreased (from 1,000 ppm to less than 5 ppm). For a feed concentration of 20,000 ppm (Figures 20 and 22), a slight increase in the air inlet temperature of only 16°C significantly affected the rate at which the catalyst responded to the concentration pulse. At 315°C, the catalyst did not light-off; i.e., the conversion of hydrogen cyanide was insignificant; while at 331°C, the catalyst rapidly lit off, such that greater than 99.9% of the challenge dose was oxidized during the exposure.

Reaction Products During Transient Testing: Reaction products formed during the transient testing were evaluated in real-time. The MSD, used to monitor the real-time concentration of hydrogen cyanide, could not be used to monitor any of the reaction products. This was due to interference of parent ions with fragments. The NO$_x$ reaction products were assessed using the NO$_x$ analyzer. This required two individual runs to be performed at the same set of process conditions in order to collect the required data. The first run was performed with the NO$_x$ analyzer in the NO mode, and the second run was performed with the NO$_x$ analyzer in the NO$_x$ mode. Results obtained from the two runs were then combined. The concentration of N$_2$ plus N$_2$O was determined by closing the material balance. That is to say, the atomic nitrogen not detected as NO$_x$ was assumed to be present as N$_2$ or N$_2$O.

Figures 24 through 29 report the reaction products and reaction product selectivity as a function of time for the oxidation of hydrogen cyanide as a function of temperature and concentration. Figure 24 reports the reaction product distribution during the oxidation of 10,000 ppm hydrogen cyanide at 310°C. Initially, the selectivity towards the
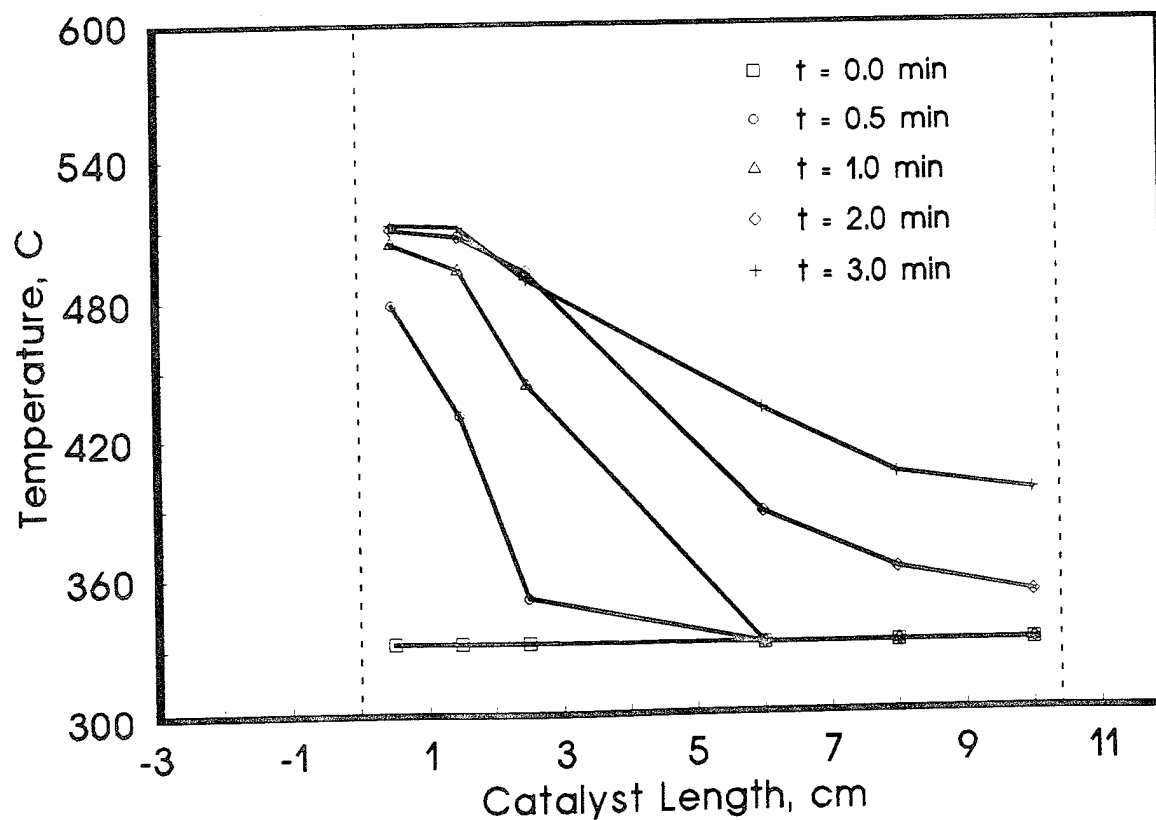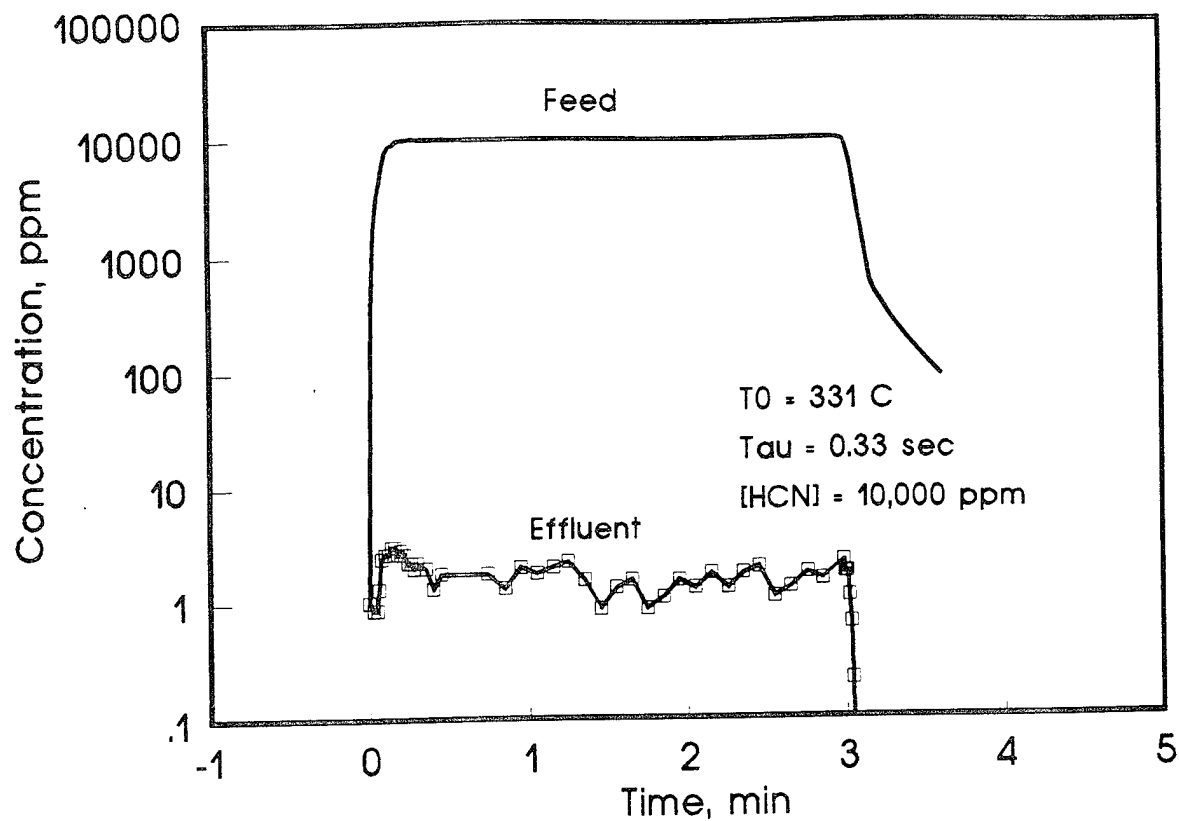
Figure 21: Feed and Effluent Concentration of Hydrogen Cyanide as a Function of Time (Top) and Catalyst Temperature Profile at Discrete Times (Bottom) Recorded During a Pulse Challenge of Hydrogen Cyanide. Temperature = 331°C, [HCN] = 10,000 ppm, τ = 0.33 s.
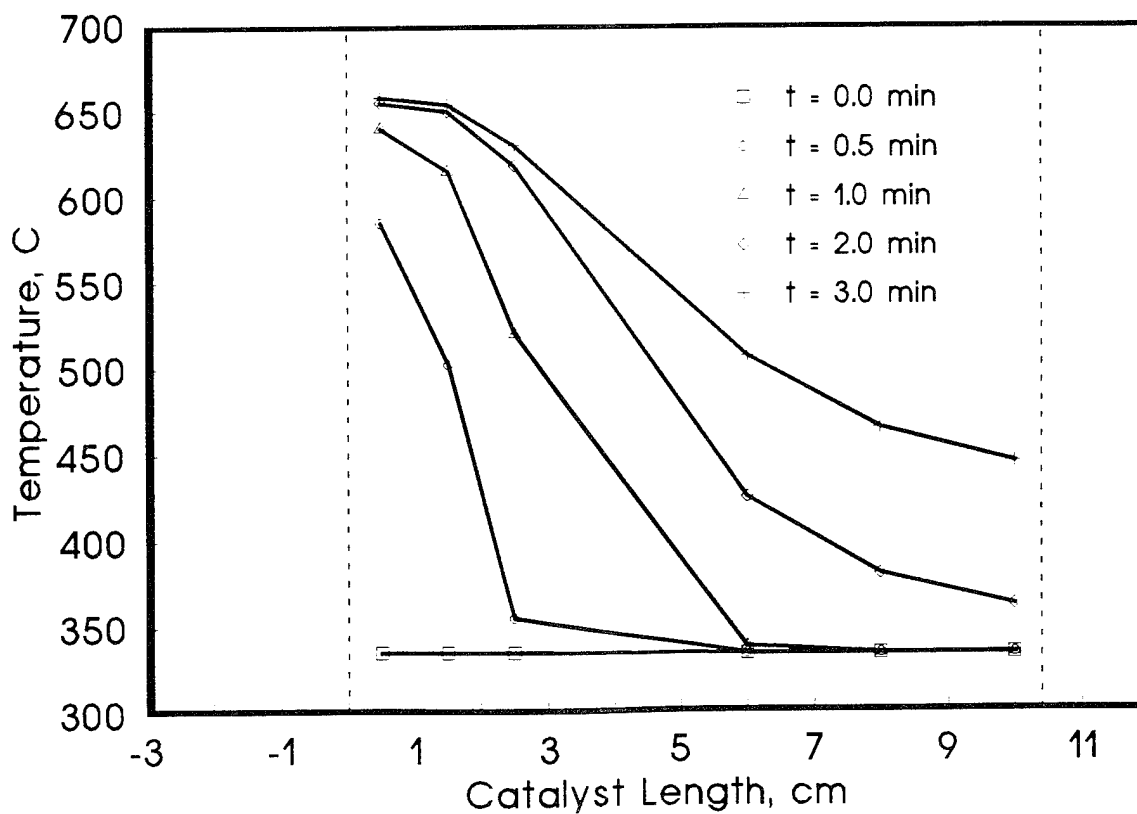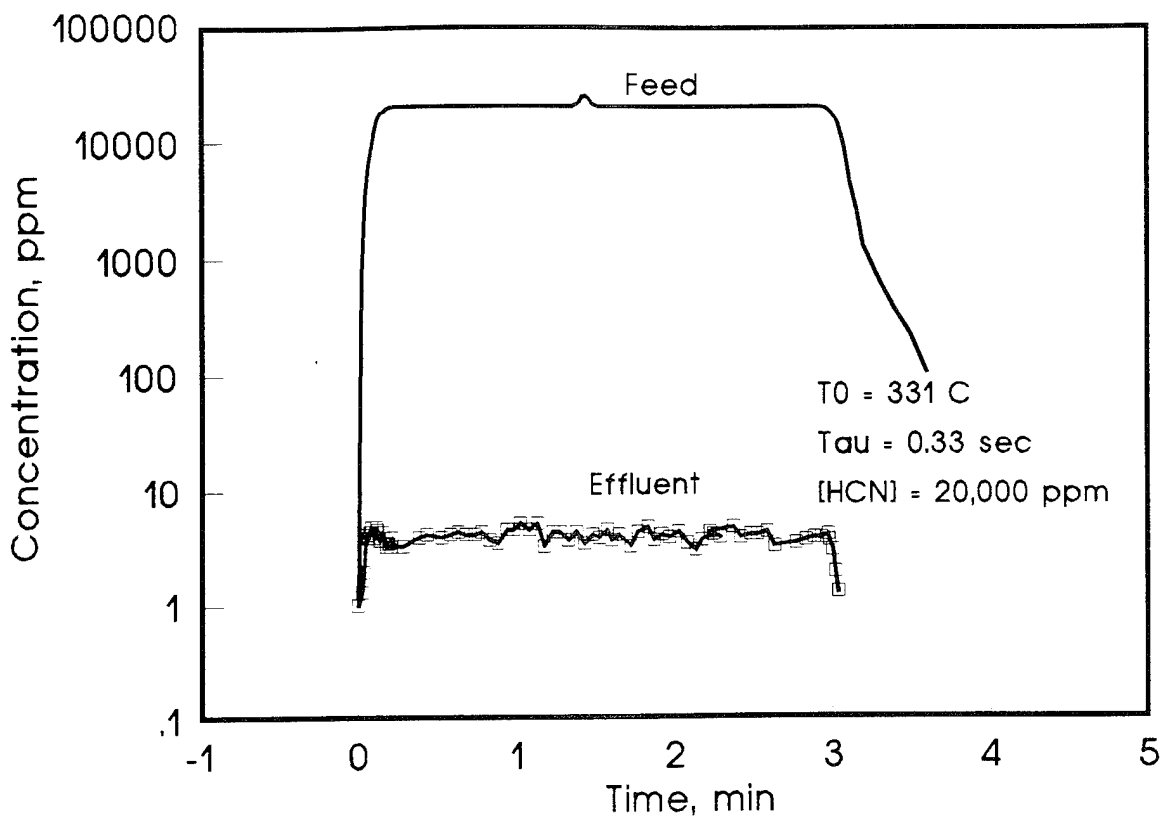
42

Figure 22: Feed and Effluent Concentration of Hydrogen Cyanide as a Function of Time (Top) and Catalyst Temperature Profile at Discrete Times (Bottom) Recorded During a Pulse Challenge of Hydrogen Cyanide. Temperature = 331°C, [HCN] = 20,000 ppm, τ = 0.33 s.
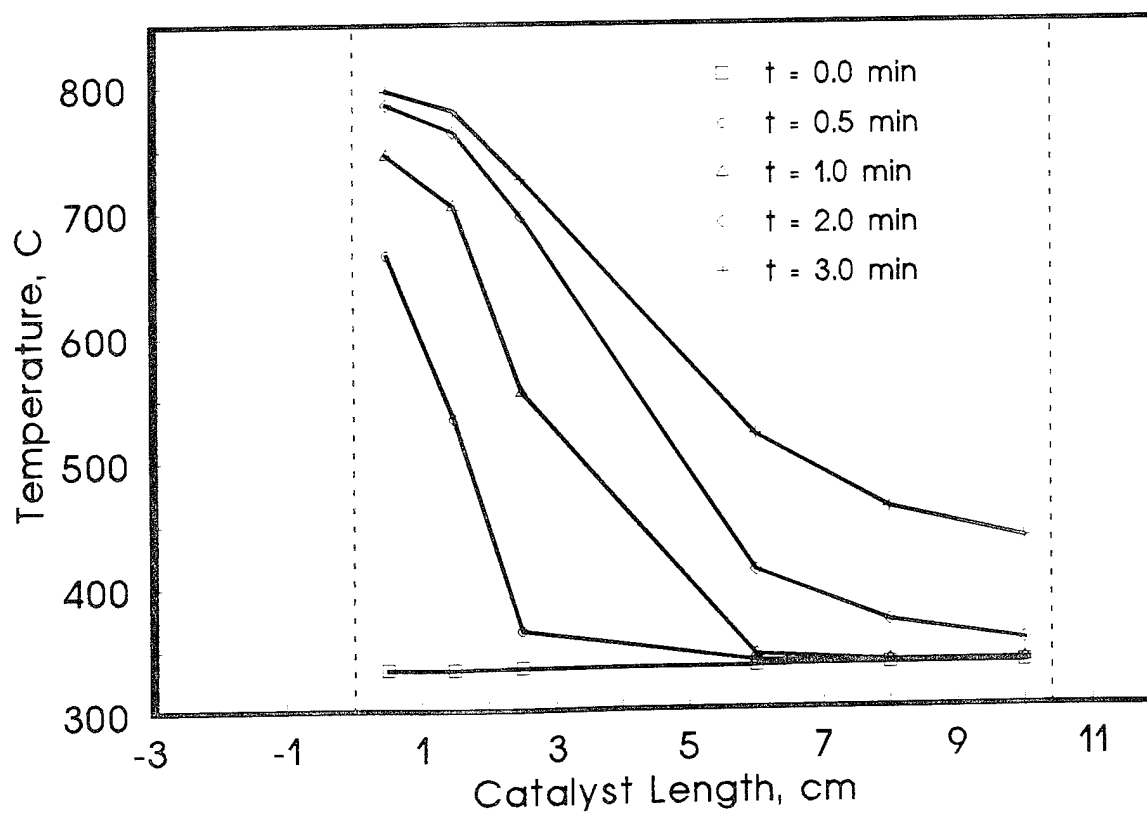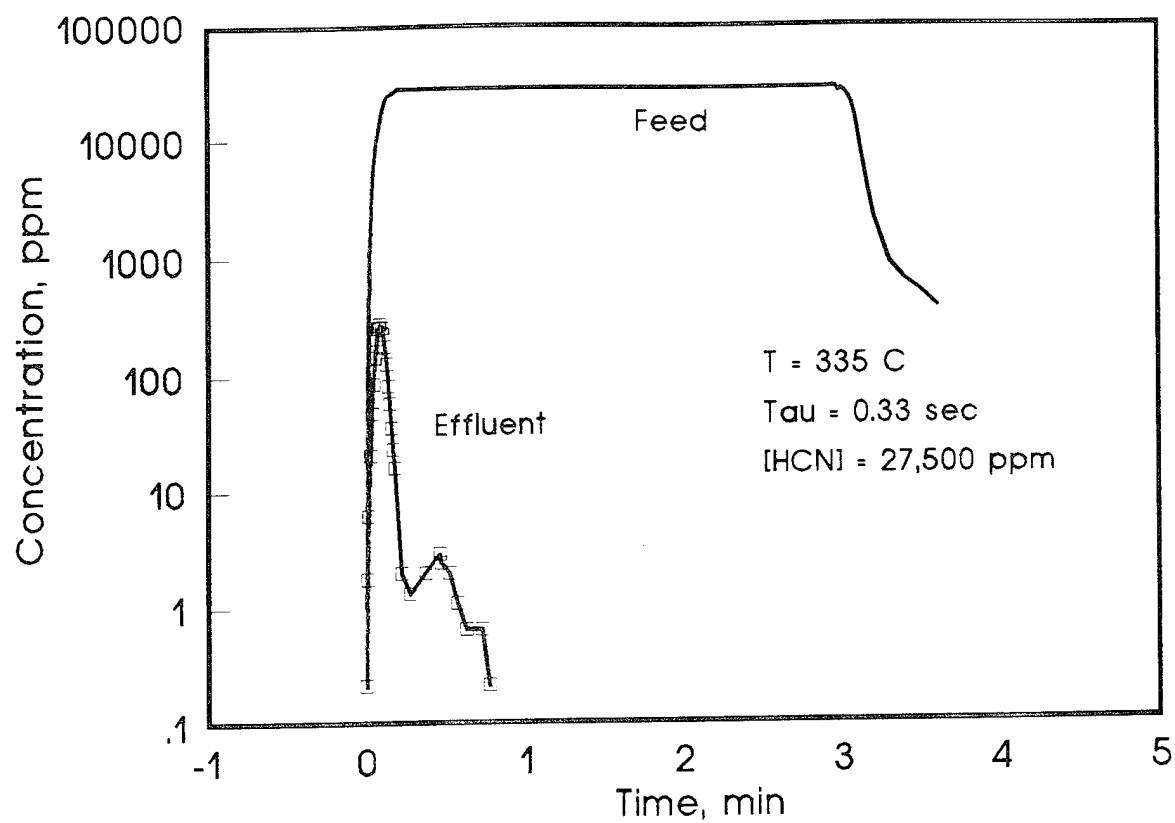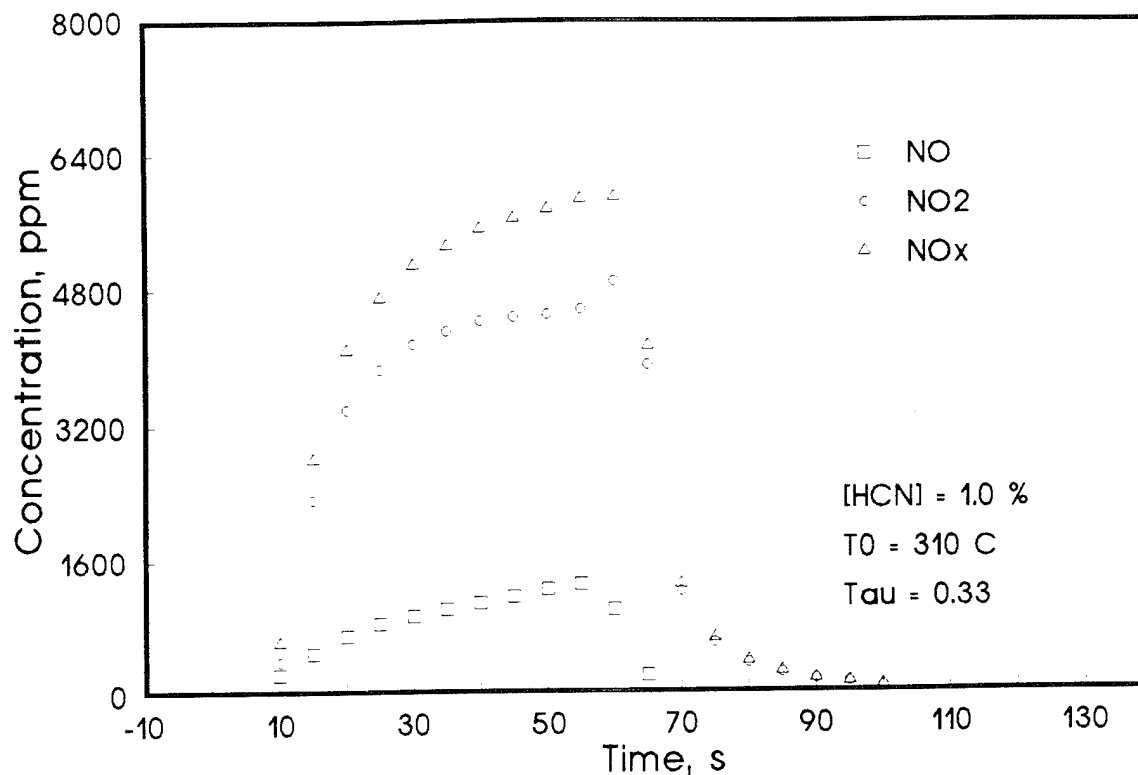
43

Figure 23: Feed and Effluent Concentration of Hydrogen Cyanide as a Function of Time (Top) and Catalyst Temperature Profile at Discrete Times (Bottom) Recorded During a Pulse Challenge of Hydrogen Cyanide. Temperature = 335°C, [HCN] = 27,500 ppm, τ = 0.33 s.

44

Reaction Products, Run HCN61,62

NO

NO2

NOx

[HCN] = 1.0 %

T0 = 310 C

Tau = 0.33

Product Selectivity, Run HCN61,62

N2 + N2O

NO

NO2

NOx

[HCN] = 1.0 %

T0 = 310 C

Tau = 0.33

Figure 24: NO$_x$ Concentrations as a Function of Time (Top) and Nitrogen Containing Reaction Product Selectivity (Bottom) as a Function of Time During a Pulse Challenge of Hydrogen Cyanide. Temperature = 310˚C, [HCN] = 10,000 ppm, τ = 0.33 s.

45

Reaction Products, Run HCN54,55

Concentration, ppm vs Time, s

Legend:
- NO
- NO2
- NOx

[HCN] = 0.5 %
T0 = 355 C
Tau = 0.33

Product Selectivity, Run HCN54,55

N-Product Selectivity, % vs Time, s

Legend:
- N2 + N2O
- NO
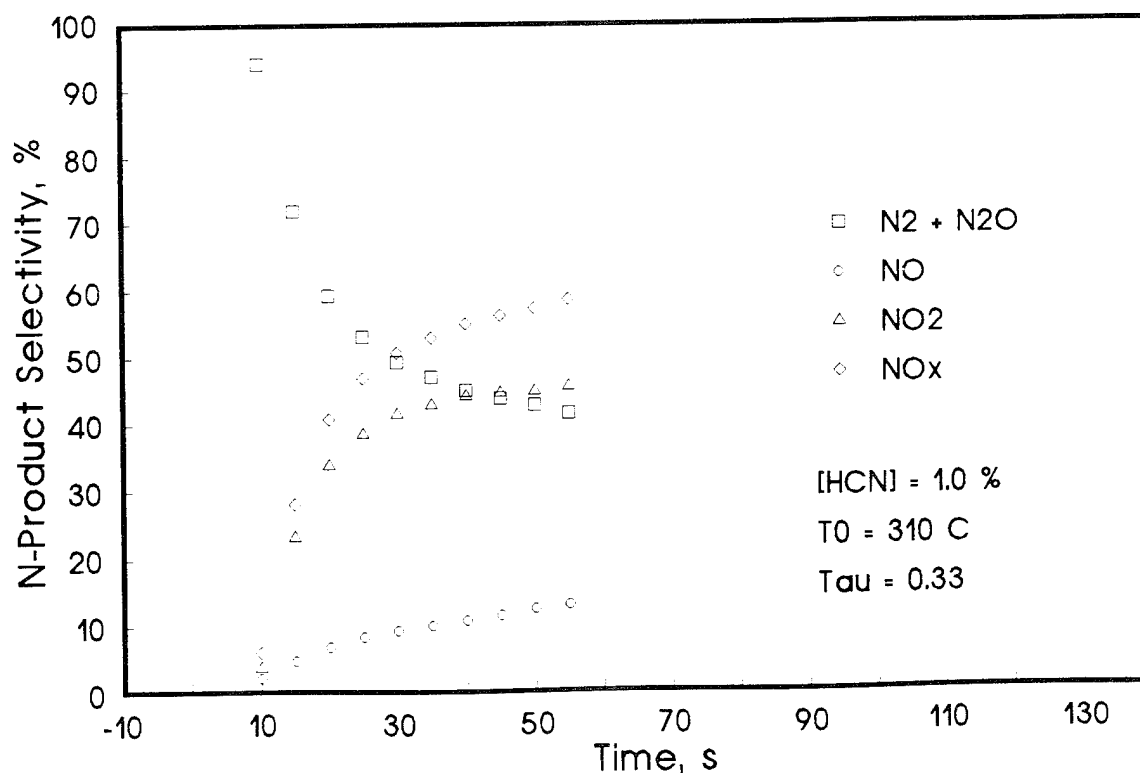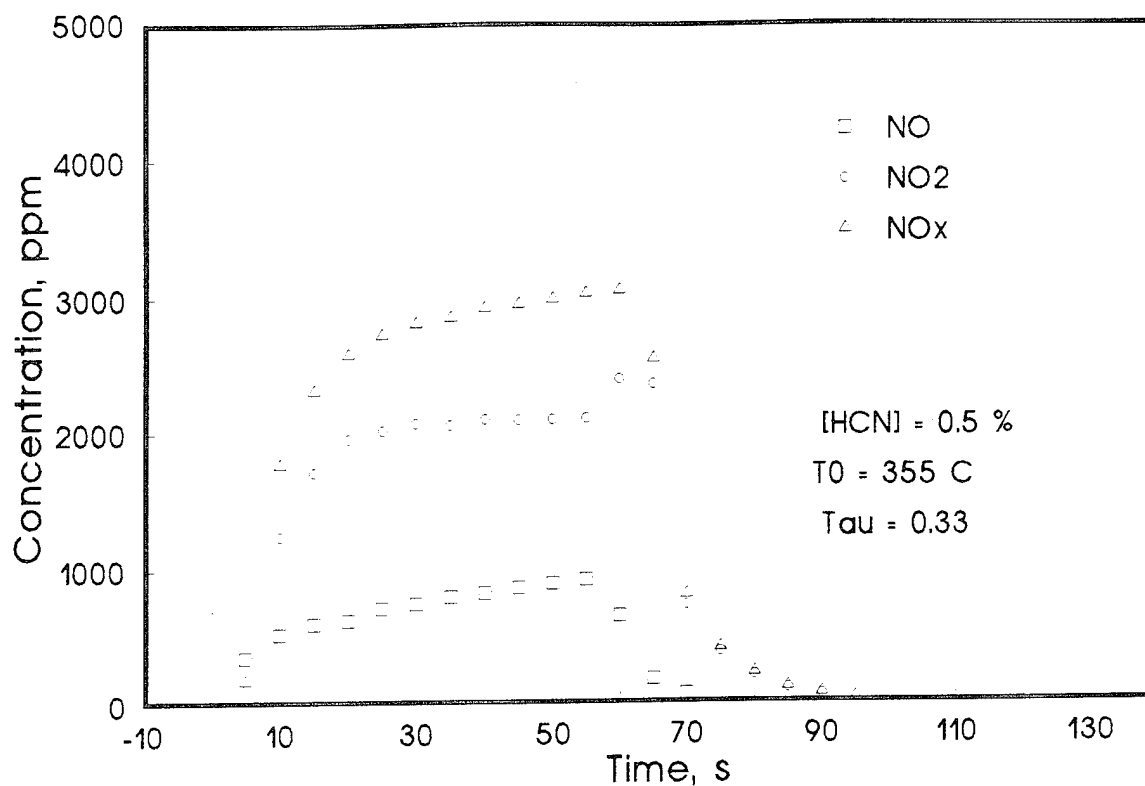- NO2
- NOx

[HCN] = 0.5 %
T0 = 355 C
Tau = 0.33

Figure 25: NO_x Concentrations as a Function of Time (Top) and Nitrogen Containing Reaction Product Selectivity (Bottom) as a Function of Time During a Pulse Challenge of Hydrogen Cyanide. Temperature = 355°C, [HCN] = 5,000 ppm, $\tau = 0.33$ s.

Reaction Products, Run HCN52,53
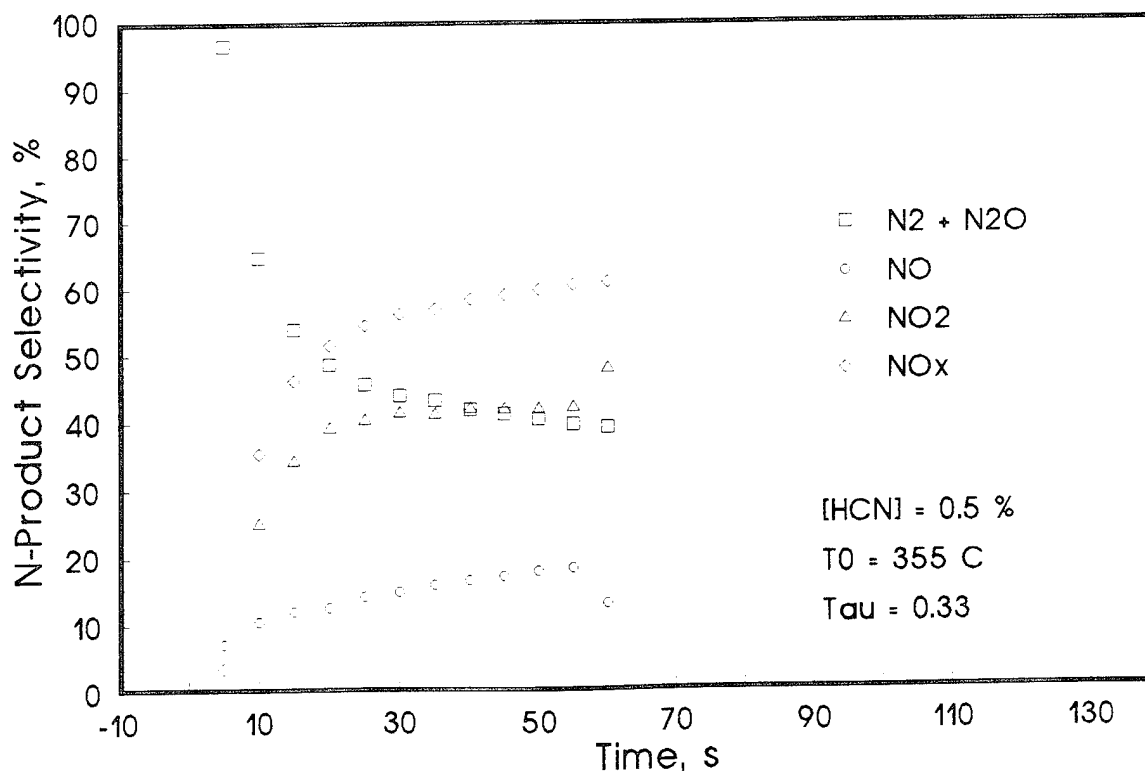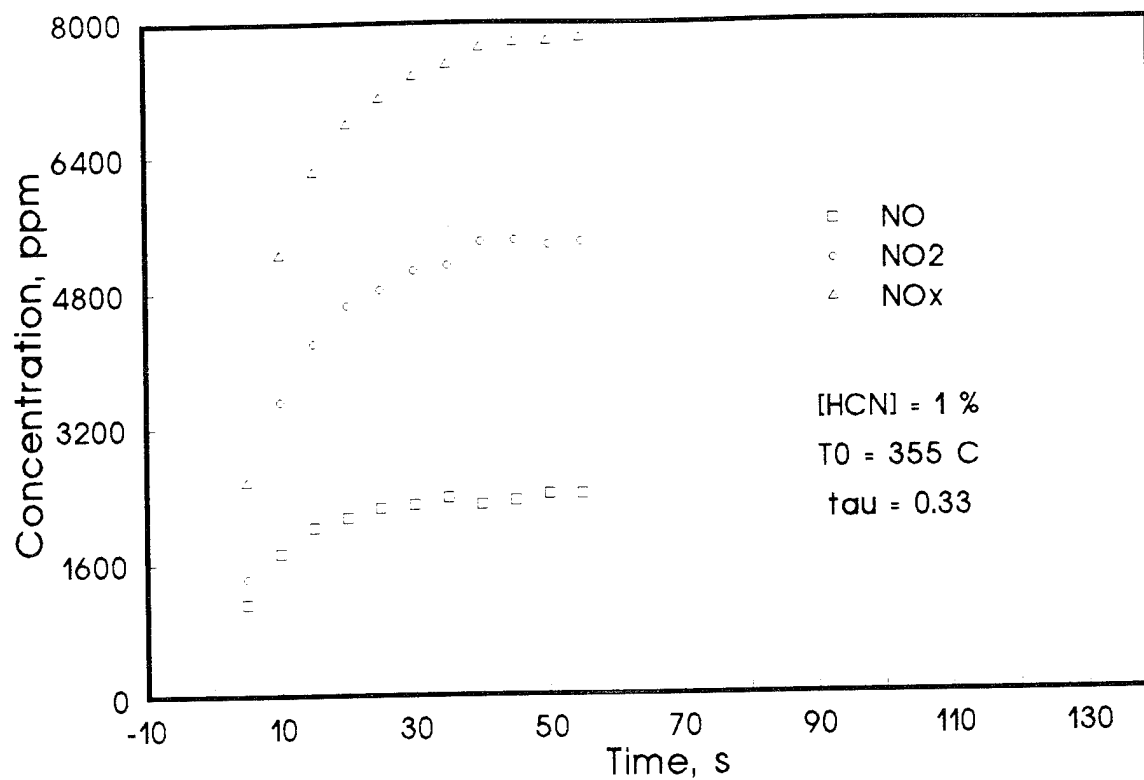

Product Selectivity, Run HCN52,53

Figure 26: NO_x Concentrations as a Function of Time (Top) and Nitrogen Containing Reaction Product Selectivity (Bottom) as a Function of Time During a Pulse Challenge of Hydrogen Cyanide. Temperature = 355°C, [HCN] = 10,000 ppm, τ = 0.33 s.

Reaction Products, Run HCN50,51

Figure data: Concentration, ppm vs Time, s

Legend:
- □ NO
- ○ NO2
- △ NOx

[HCN] = 2 %
T0 = 355 C
tau = 0.33

Product Selectivity, Run HCN50,51

Figure data: N-Product Selectivity, % vs Time, s

Legend:
- □ N2 + N2O
- ○ NO
- △ NO2
- < NOx

[HCN] = 2 %
T0 = 355 C
tau = 0.33

Figure 27: NO_x Concentrations as a Function of Time (Top) and Nitro
Reaction Product Selectivity (Bottom) as a Function of Time During a Pu
Hydrogen Cyanide. Temperature = 355°C, [HCN] = 20,000 ppm, τ = 0.3

Reaction Products, Run HCN63,64

Legend:
- □ NO
- ○ NO2
- △ NOx

[HCN] = 1.0 %
T0 = 400 C
Tau = 0.33

Product Selectivity, Run HCN63,64

Legend:
- □ N2 + N2O
- ○ NO
- △ NO2
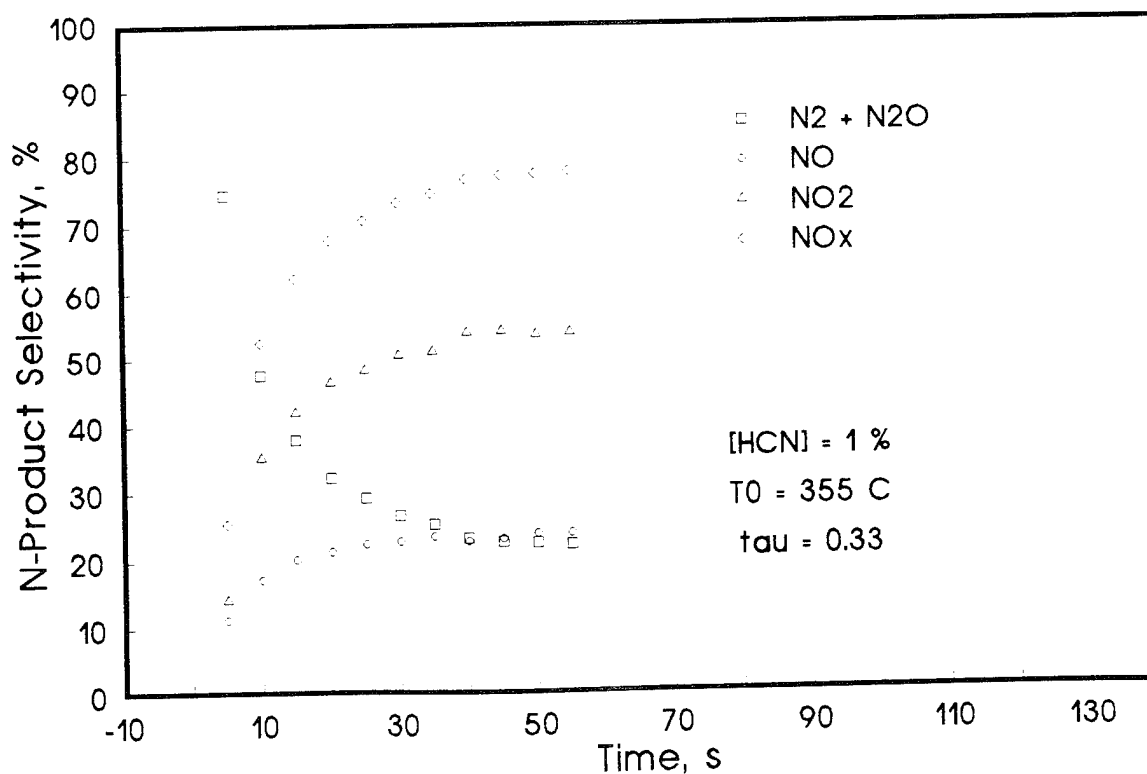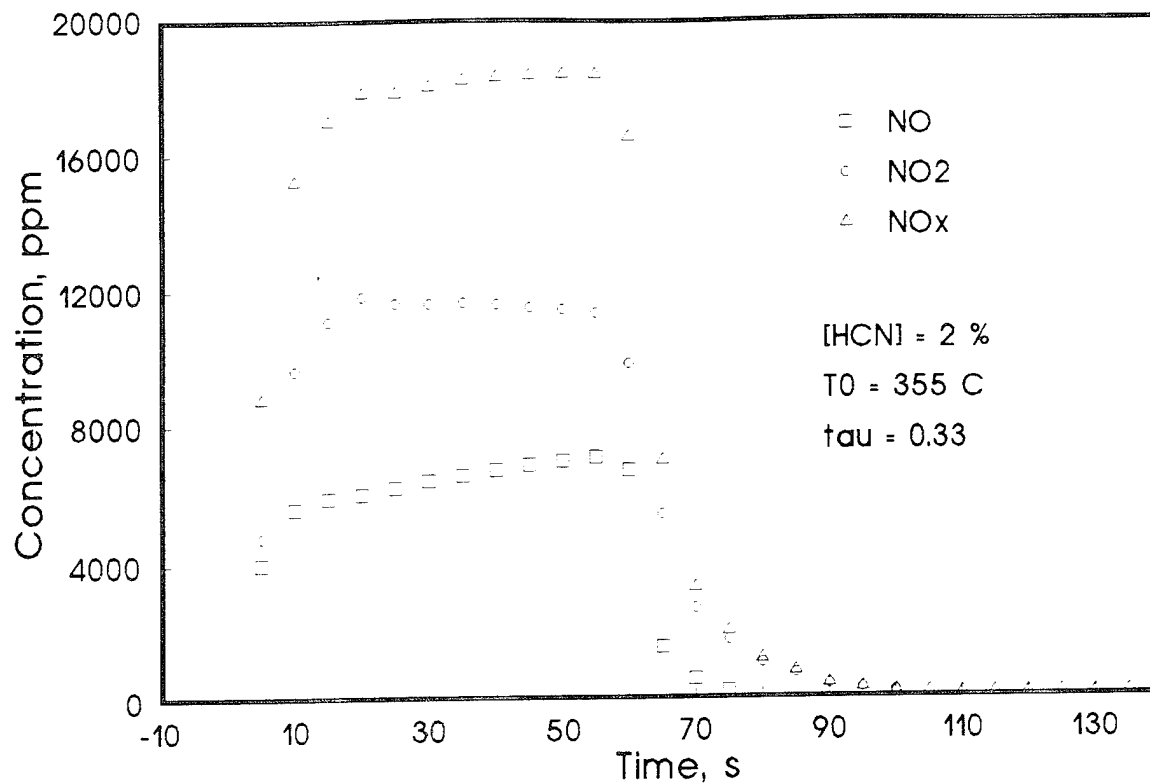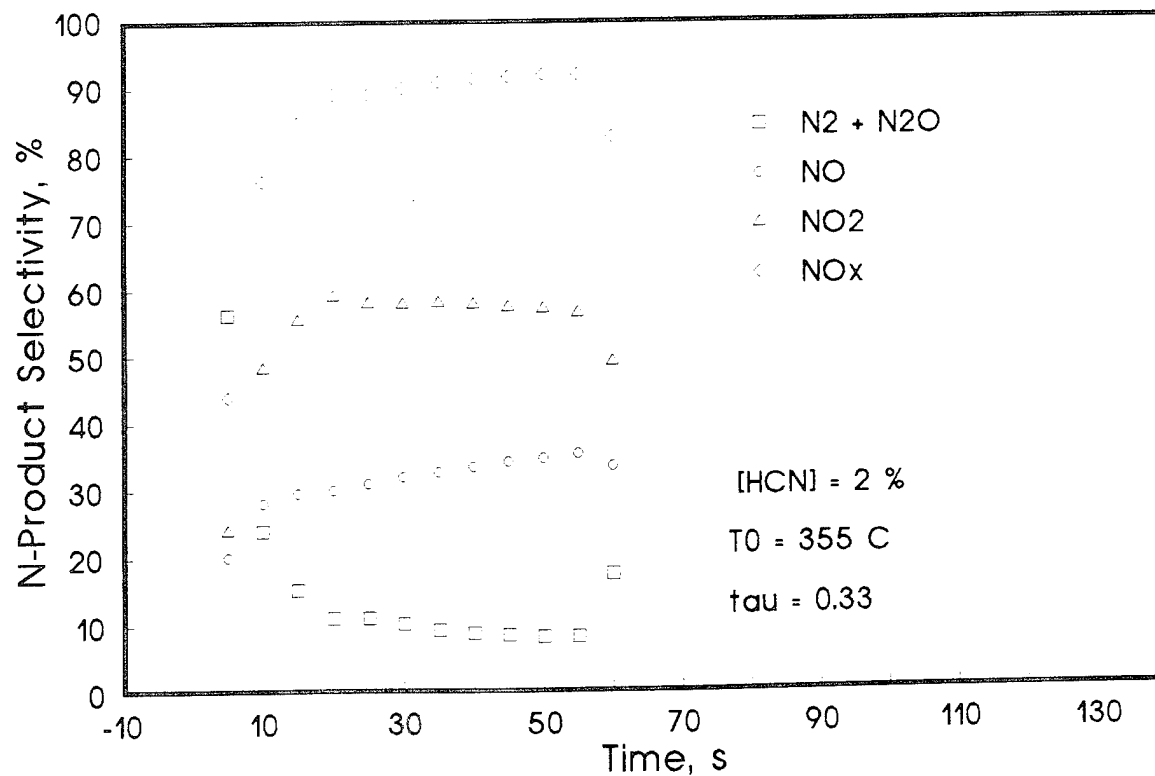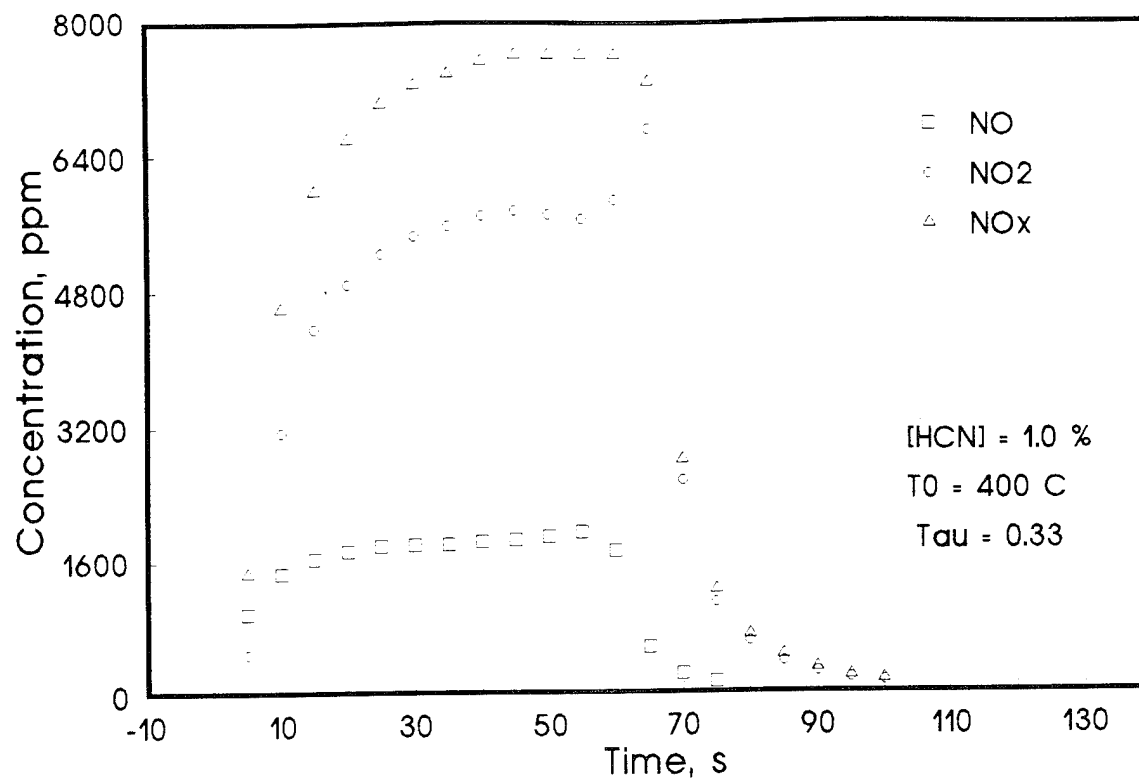- ○ NOx

[HCN] = 1.0 %
T0 = 400 C
Tau = 0.33

Figure 28: NO_x Concentrations as a Function of Time (Top) and Nitrogen Containing Reaction Product Selectivity (Bottom) as a Function of Time During a Pulse Challenge of Hydrogen Cyanide. Temperature = 400°C, [HCN] = 10,000 ppm, τ = 0.33 s.

49

Reaction Products, Run HCN65,66

Concentration, ppm vs Time, s

[HCN] = 2.0 %

T0 = 400 C

Tau = 0.33

- □ NO
- ○ NO2
- △ NOx

Product Selectivity, Run HCN65,66

N-Product Selectivity, % vs Time, s

[HCN] = 2.0 %

T0 = 400 C

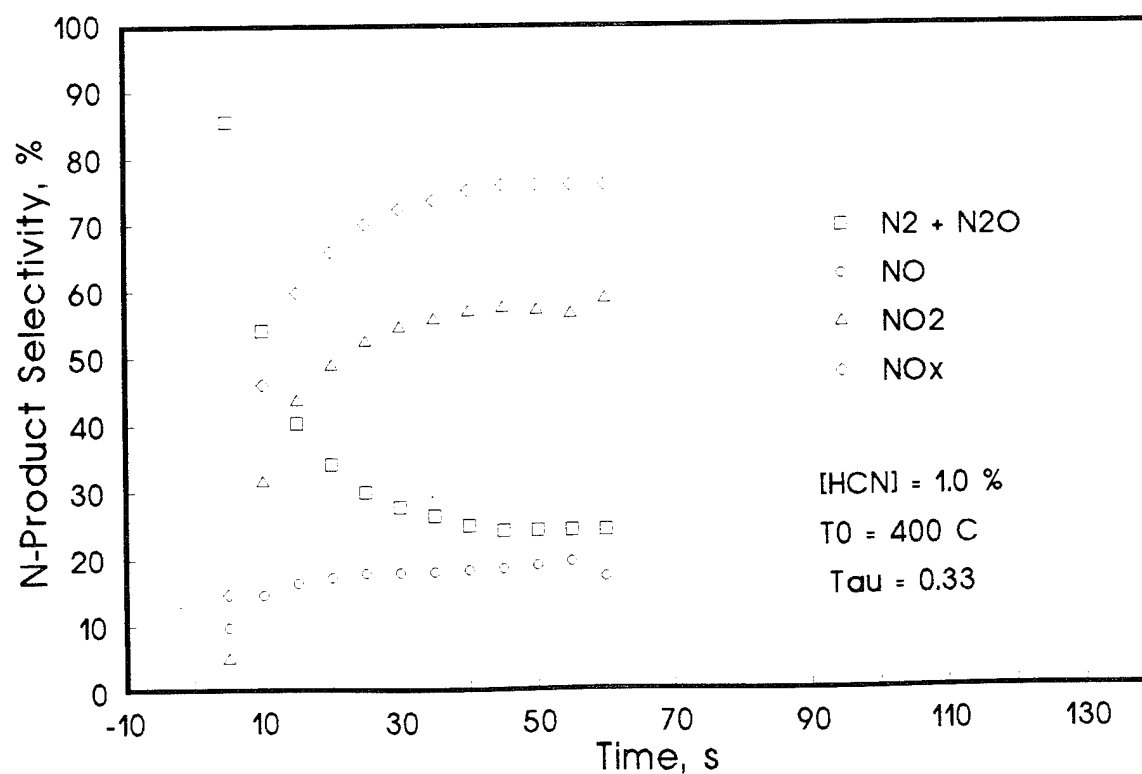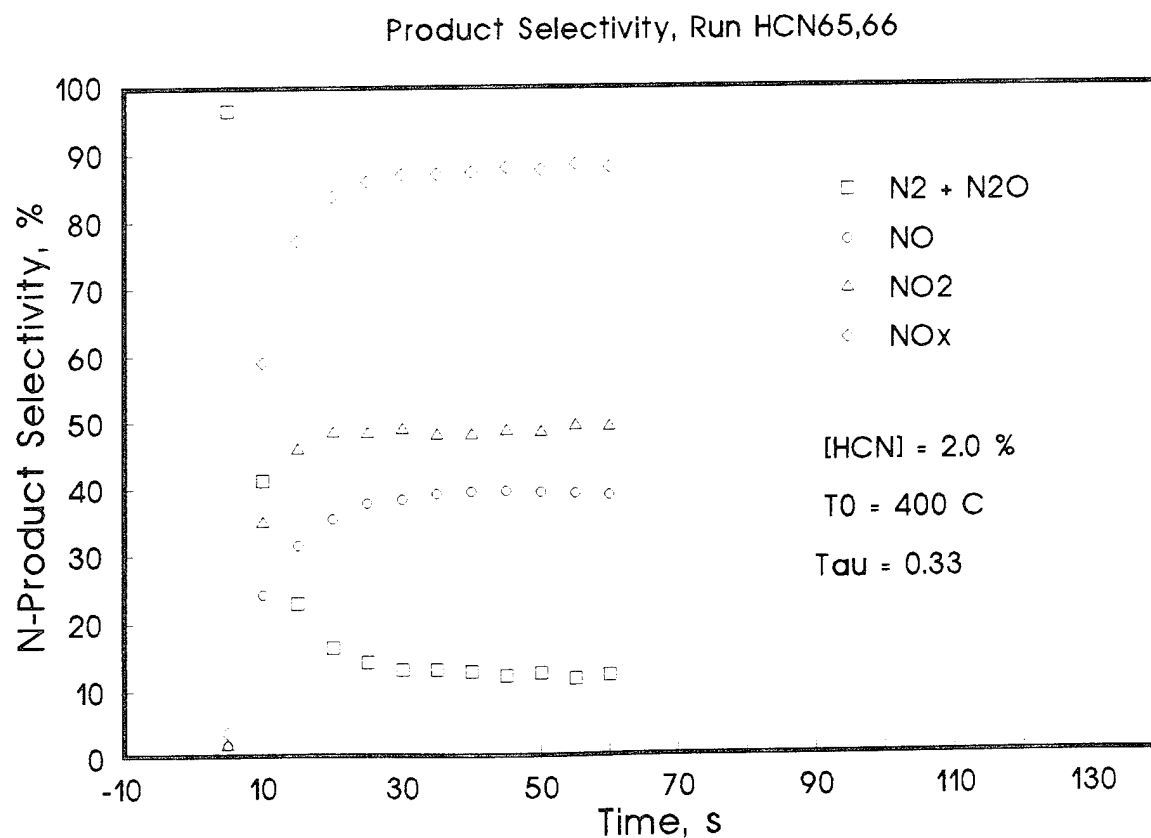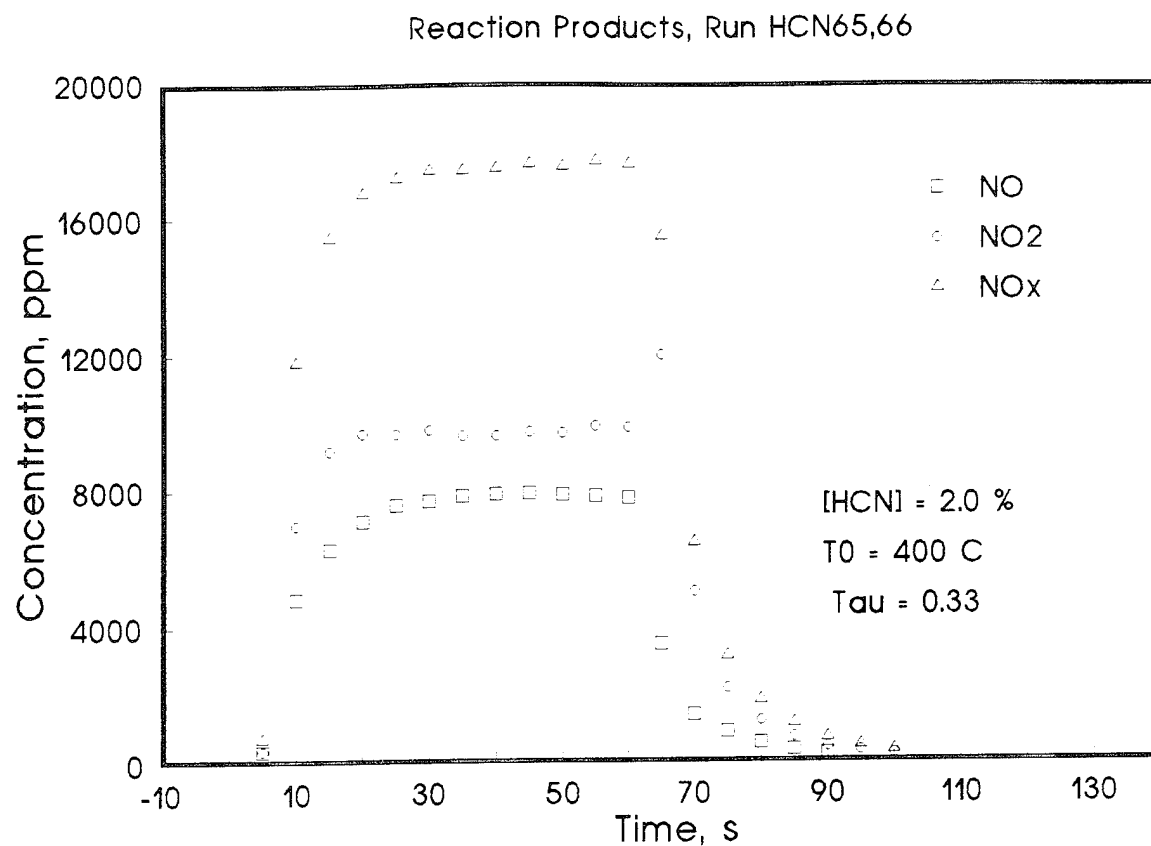Tau = 0.33

- □ N2 + N2O
- ○ NO
- △ NO2
- ◁ NOx

Figure 29: NO_x Concentrations as a Function of Time (Top) and Nitrogen Containing Reaction Product Selectivity (Bottom) as a Function of Time During a Pulse Challenge of Hydrogen Cyanide. Temperature = 400°C, [HCN] = 20,000 ppm, τ = 0.33 s.

reduced products is greater than 90%. However, the selectivity towards the formation of the reduced products decreases sharply over the first 20-30 seconds of the run in favor of the formation of NO_x. As discussed previously, the catalyst temperature increases rapidly during the hydrogen cyanide challenge. The increase in temperature, as shown in Figure 5, shifts the reaction product distribution towards the formation of NO_x. Hence, even though the initial product distribution is favorable, the light-off behavior of the catalyst shifts the product distribution such that the yield of NO_x becomes significant.

Figures 25 through 27 illustrate the effects of hydrogen cyanide concentration on the reaction product distribution for runs conducted at 355°C. Increasing the concentration results in increasing the NO_x selectivity. Note that the final NO_x selectivity increases from 60 to 90% as the hydrogen cyanide concentration is increased from 5,000 to 20,000 ppm. The reason for the observed increased NO_x selectivity may be attributed to an increase in the catalyst temperature during the challenge. Increasing the feed concentration from 5,000 to 20,000 ppm results in increasing the maximum catalyst temperature from 450 to 850°C. Similar nitrogen selectivity data are illustrated in Figures 28 and 29 for data recorded at 400°C.

5. CONCLUSIONS

Hydrogen cyanide may be readily oxidized over the monolithic oxidation catalyst at temperatures greater than about 330°C. The presence of water vapor in the feed was found to have no effect on the catalytic activity. Reaction products consisted of CO_2, N_2, N_2O, NO and NO_2, with the nitrogen product selectivity being a strong function of catalyst temperature. Catalytic deactivation was not observed, indicating that the catalyst is very stable. Under isothermal conditions, the oxidation of hydrogen cyanide could be modeled employing a reaction mechanism which assumes the rate limiting step to be a reaction between adsorbed hydrogen cyanide and adsorbed oxygen. Results of the pulse testing reveal that transient effects are significant. Given a sufficient air inlet temperature, the catalyst rapidly lights-off, minimizing the dose of hydrogen cyanide which elutes through the filter. The transient behavior of the catalyst was found to be a strong function of temperature and concentration. Reaction products observed during the transient testing consisted primarily of NO_x, due to the large adiabatic temperature rise.

Blank

LITERATURE CITED

1) Rossin, J.A., E. Petersen, D. E. Tevault, R. Lamontagne and L. Isaacson, "Effects of Environmental Weathering on the Properties of ASC Whetlerite," *Carbon*, **29**, 197 (1991).

2) Latimer, W. M., *Military Problems with Aerosols and Nonpersistent Gases*; National Defense Research Committee Report, Div. 10: Washington, D.C. 1946.

3) "1992-93 Threshold Limit Values for Chemical Substances and Physical Vapors," Am. Conf. Ind. Hygiene., 1992.

4) Klinghoffer, A. A. and J. A. Rossin, *Effects of Process Conditions on the Transient Response of a Monolithic Oxidation Catalyst*, in Environmental Catalysts (J. Armor, ed.), ACS Symp. Ser., 1993 (in press).

5) Gland, J. L.; Sexton, B. A.; Fisher, G. B. Oxygen Interactions with the Pt(111) Surface. *Surf. Sci.* **1980**, *95*, 587.

6) Froment, G. F. and K. B. Bischoff, Chemical Reactor Analysis and Design; Wiley: New York, 1979.

7) Irandoust, S. and B. Andersson, "Monolithic Catalysts for Nonautomobile Applications," *Catal. Rev. Sci. Eng.*, **30**, 341 (1988).